Expectation Maximization for Clustering on Hyperspheres

Arindam Banerjee[*] Inderjit Dhillon[†] Joydeep Ghosh[*] Suvrit Sra[†]

28 February 2003[‡]

Technical Report # TR-03-07

Abstract

High dimensional directional data is becoming increasingly important in contemporary applications such as analysis of text and gene-expression data. A natural model for multi-variate directional data is provided by the von Mises-Fisher (vMF) distribution on the unit hypersphere that is analogous to multi-variate Gaussian distribution in $\mathbb{R}^d$. In this paper, we propose modeling complex directional data as a mixture of vMF distributions. We derive and analyze two variants of the Expectation Maximization (EM) framework for estimating the parameters of this mixture. We also propose two clustering algorithms corresponding to these variants. An interesting aspect of our methodology is that the spherical kmeans algorithm (kmeans with cosine similarity) can be shown to be a special case of both our algorithms. Thus, modeling text data by vMF distributions lends theoretical validity to the use of cosine similarity which has been widely used by the information retrieval community. We provide several results on modeling high-dimensional text and gene data as experimental validation. The results indicate that our approach yields superior clusterings especially for difficult clustering tasks in high-dimensional space.

1 Introduction

Clustering or segmentation of data is a fundamental data analysis step that has been widely studied across multiple disciplines[JD88, Mac67]. However, several large datasets that are being acquired from scientific domains, as well as the world wide web, have a variety of complex characteristics that severely challenge traditional methods for clustering. These large datasets also impose demands on the evaluation, scalability and visualization of results [Gho03]. This article is concerned with the clustering of high-dimensional directional data that is becoming increasingly common in several application domains.

One can broadly categorize clustering approaches into *generative* and *discriminative* ones. In a generative approach [Smy97, Bil98, Ros98, JH99], the data is modeled as being generated by an underlying parametric, probabilistic process. Values for the parameters are estimated from the input data, and properties of the clusters are then inferred from these parameters. Discriminative approaches [Vap98, SS01, Ind99], on the other hand, make no assumptions whatsoever about how the data points were generated. Instead, they assume that a well defined distance or similarity measure exists between any pair of objects. The clustering process is then essentially an attempt

[*] Department of E.C.E., Univ. of Texas at Austin

[†] Department of Comp. Sci., Univ. of Texas at Austin

[‡] Revised 8th June 2003.

to partition the objects so that intra-partition (within cluster) dissimilarities are smaller than inter-partition (across clusters) dissimilarities[1].

The performance of an approach (and of a specific method within that approach) is quite data dependent; there is no clustering method that works the best across all types of data distributions. Generative models, however, often provide better insight into the nature of the clusters. From an application point of view, a lot of domain knowledge can be incorporated into the generative models so that clustering of data brings out specific desirable patterns that one is looking for. It is for this reason that the generative (parametric) approach is referred to as the method of particular inference in statistical learning theory [Vap98].

Clustering algorithms using the generative model framework, often involve an appropriate application of the Expectation Maximization (EM) algorithm [DLR77, Col97] on a properly chosen statistical generative model for the data under consideration. At present, for vector data, there are well studied clustering algorithms for popular generative models such as a mixture of Gaussians, whose effect is analogous to the use of Euclidean or Mahalanobis type distances from the discriminative perspective. However, in many cases such distances are not appropriate, e.g., from empirical studies in information retrieval applications, *cosine similarity* has been found to be a good measure of similarity for analyzing and clustering text documents. Thus, some domains require the use of *directional data*[MJ00] — data in which only the direction of the vectors is considered and all the vectors involved have unit Euclidean norm. In fact several large, high-dimensional datasets exhibit directional characteristics. These motivations suggest the need for generative models that are more appropriate for the analysis and clustering of directional data. In this article, we present a generative mixture model for directional data on the unit hypersphere and derive two clustering algorithms using this mixture model. We show the connection between the proposed algorithms and a class of existing algorithms for clustering high-dimensional directional data, and present detailed experimental comparisons among them.

In order to motivate our work, we present examples of a few important domains where directional data is becoming increasingly common. One such domain is text analysis, and text clustering in particular. It has been experimentally demonstrated that in order to remove the biases arising from the length of a document, it often helps to normalize the data vectors [DM01]. Note that running a clustering algorithm such as `kmeans` [DHS00, Mac67] on normalized data so that the total *Euclidean distortion* in the data with respect to the cluster representative is minimized, is not a reasonable idea since the Euclidean distortion is not a natural measure of dispersion for normalized data. On the other hand, if the cluster representatives themselves are normalized, then the Euclidean distortion (chordal distance) is negatively proportional to the *cosine similarity* in the data with respect to the cluster representative. Given $\mathbf{x}, \mathbf{y} \in \mathbb{R}^d$ such that $\|\mathbf{x}\| = \|\mathbf{y}\| = 1$, we have

$$\|\mathbf{x} - \mathbf{y}\|^2 = \|\mathbf{x}\|^2 + \|\mathbf{y}\|^2 - 2\mathbf{x}^T\mathbf{y} = 2 - 2\mathbf{x}^T\mathbf{y},$$

where the inner product $\mathbf{x}^T\mathbf{y}$ is the so-called cosine similarity, since it equals the cosine of the angle between $\mathbf{x}$ and $\mathbf{y}$. Thus, minimizing the Euclidean distortion with respect to normalized cluster representatives is equivalent to maximizing the cosine similarity of the data points with the cluster representatives. However, note that there is a significant conceptual difference compared to the classical approach since, the representatives themselves are normalized in this case. Therefore, maximizing cosine similarity in a particular clustering scheme is tantamount to considering only the directional properties of the data. The use of cosine similarity has been shown to work well for very high-dimensional text collections [DM01, BG02, BBM02] using the standard vector-space model [FBY92, Sal89].

[1] Note that the approaches are not mutually exclusive, as `kmeans` can be seen as a member of both the approaches [KMN97].

Another domain in which directional data shows up is bioinformatics. At present, gene expression datasets are a major source of information about genes and their interactions. DNA microarrays measure the mRNA expression of all genes encoded by a genome in a single experiment [LRM$^+$97]. From these microarray experiments an expression vector for each gene is constructed. The expression vector describes the expression level of a gene subject to a range of cellular conditions, cell types, genetic backgrounds, etc. Thus analysis of gene expression data can prove to be a valuable source of information for understanding and predicting functions of genes. A fundamental analysis step is the clustering of genes that exhibit similar expression levels. Given enough independent experiments, genes clustered in this fashion tend to be functionally related[ESBB98, MPT$^+$99].

A similarity measure that has been found to be useful in the gene clustering domain is the Pearson correlation coefficient of the expression levels of genes. Given $\mathbf{x}, \mathbf{y} \in \mathbb{R}^d$, the Pearson product moment correlation between them is given by

$$\rho(\mathbf{x}, \mathbf{y}) = \frac{\sum_{i=1}^{d}(x_i - \bar{x})(y_i - \bar{y})}{\sqrt{\sum_{i=1}^{d}(x_i - \bar{x})^2} \times \sqrt{\sum_{i=1}^{d}(y_i - \bar{y})^2}}, \tag{1.1}$$

where $\bar{x} = \frac{1}{d}\sum_{i=1}^{d} x_i$, $\bar{y} = \frac{1}{d}\sum_{i=1}^{d} y_i$. Considering the mapping $\mathbf{x} \mapsto \tilde{\mathbf{x}}$ such that $\tilde{\mathbf{x}}_i = \frac{x_i - \bar{x}}{\sqrt{\sum_{i=1}^{d}(x_i - \bar{x})^2}}$, we have $\rho(\mathbf{x}, \mathbf{y}) = \tilde{\mathbf{x}}^T\tilde{\mathbf{y}}$. Thus, the Pearson correlation is exactly the cosine similarity between $\tilde{\mathbf{x}}$ and $\tilde{\mathbf{y}}$ that are obtained by a simple mapping from the given feature vectors $\mathbf{x}$ and $\mathbf{y}$. Hence, analysis and clustering of gene expression data using Pearson correlations is essentially a clustering problem using directional data. In fact, any algorithm that uses Pearson correlations, e.g., a number of standard techniques in recommender systems based on collaborative filtering [SKKR01], can be considered as a problem involving directional data and hence should be analyzed under the domain of directional statistics [MJ00].

In [DM01], the `spkmeans` algorithm for clustering spherical data was proposed. The connection between a generative model involving von Mises-Fisher distributions and the `spkmeans` algorithm was first observed in [BG02]. In this article, we propose a mixture model on the unit hypersphere for modeling directional data based on the von Mises-Fisher (vMF) distribution and derive two EM-based clustering algorithms based on the same. To this end, we first present the vMF distribution on the sphere and discuss the maximum likelihood parameter estimates for a single vMF in section 2. In section 3, we introduce the generative model for a mixture of vMF distributions and analyze the maximum likelihood parameter estimates of the mixture model from a given dataset using the EM framework. Based on the analysis in section 3, two clustering algorithms, using soft- and hard-assignments respectively, are proposed in section 4. We show the connection of the proposed algorithms to the `spkmeans` algorithm in section 4.1. A brief discussion of the numerical implementation issues is in section 4.2. A summary of artificial and real life datasets used for experimentation is presented in section 5. We discuss the experimental results on various datasets in section 6. Some limitations of our present approach and the clustering process in general are discussed in section 7. Section 8 presents concluding remarks and outlines directions for future work.

A word about the notation: bold faced variables, e.g., $\mathbf{x}$, $\boldsymbol{\mu}$, represent vectors; $\|\cdot\|$ denotes the L_2 norm; sets are represented by calligraphic upper-case letter, e.g., $\mathcal{X}$, $\mathcal{Z}$; $\mathbb{R}$ denotes the set of reals; $\mathbb{S}^{d-1}$ denotes the $(d-1)$-dimensional unit hypersphere embedded in $\mathbb{R}^d$. Probability density functions are denoted by lower case alphabets, e.g., f, p; probability of sets of events is denoted by capital letter, e.g., P, Q. If a random variable z is distributed as p, we denote this by $\mathrm{z} \sim p$. Expectation of functions of a random variable $\mathrm{z} \sim p$ are denoted by $E_{\mathrm{z}\sim p}[\cdot]$, or, simply $E_p[\cdot]$ if the random variable is distributed as p. Unless otherwise mentioned, we study data that lies on the unit hypersphere, i.e., is L_2-normalized — we use the terms "directional data" and "spherical data" interchangeably when talking about such data.

2 The von Mises-Fisher (vMF) distribution

A d-dimensional unit random vector $\mathbf{x}$ (i.e., $\|\mathbf{x}\| = 1$) is said to have d-variate von Mises-Fisher (vMF) distribution $M_d(\boldsymbol{\mu}, \kappa)$, if its probability density function is given by:

$$f(\mathbf{x}|\boldsymbol{\mu}, \kappa) = c_d(\kappa) e^{\kappa \boldsymbol{\mu}^T \mathbf{x}} \qquad \mathbf{x}, \boldsymbol{\mu} \in \mathbb{S}^{d-1} \subseteq \mathbb{R}^d,\ \kappa \in \mathbb{R}_+ \cup \{0\}. \tag{2.1}$$

The normalizing constant $c_d(\kappa)$ is given by (see [DS03] for detailed derivations)

$$c_d(\kappa) = \frac{\kappa^{d/2-1}}{(2\pi)^{d/2} I_{d/2-1}(\kappa)}, \tag{2.2}$$

where $I_r(\kappa)$ represents the modified Bessel function of the first kind of order r and argument κ (see [AS74] for more on Bessel functions). The distribution $M_d(\boldsymbol{\mu}, \kappa)$ is parameterized by the mean direction $\boldsymbol{\mu}$, and the concentration parameter κ, so-called because it characterizes how strongly the unit vectors following $M_d(\boldsymbol{\mu}, \kappa)$ are concentrated about the mean direction $\boldsymbol{\mu}$. Larger values of κ imply stronger concentration about the mean direction. In particular when $\kappa = 0$, $M_d(\boldsymbol{\mu}, \kappa)$ reduces to the uniform distribution on $\mathbb{S}^{d-1}$, and as $\kappa \to \infty$, $M_d(\boldsymbol{\mu}, \kappa)$ tends to a point distribution concentrated at $\boldsymbol{\mu}$.

The von Mises-Fisher distribution is natural for directional data and has properties analogous to those of the multi-variate normal distribution in $\mathbb{R}^d$. Mardia and Jupp [MJ00] mention that the density on $\mathbb{S}^{d-1}$ that maximizes the entropy, while keeping $E[\mathbf{x}]$ fixed, is a vMF density. See Rao [Rao73, pp. 172–174] and Mardia [Mar75] for a proof. A maximum likelihood characterization says: let $f(\mathbf{x}; \boldsymbol{\mu})$ be a probability density function on $\mathbb{S}^{d-1}$ with mean direction $\boldsymbol{\mu}$ and $E[\mathbf{x}] = \zeta \boldsymbol{\mu}$ where $\zeta > 0$. If for all random samples the sample mean direction is a maximum likelihood estimate (m.l.e.) of $\boldsymbol{\mu}$ and $f(\mathbf{x}; \boldsymbol{\mu}) = g(\mathbf{x}^T \boldsymbol{\mu})$ for all $\mathbf{x} \in \mathbb{S}^{d-1}$, where the function g is lower semi-continuous from the left at 1, then $f(\mathbf{x}; \boldsymbol{\mu})$ is a von Mises-Fisher density. Various other results related to the vMF density and its genesis are given in [MJ00].

2.1 Maximum Likelihood Estimates

We now briefly discuss the maximum likelihood estimation of the parameters of a single vMF distribution from a given data set. Let $\mathcal{X}$ be a finite set of sample unit vectors drawn independently following $M_d(\boldsymbol{\mu}, \kappa)$, i.e., we have

$$\mathcal{X} = \{\mathbf{x}_i \mid \mathbf{x}_i \sim M_d(\boldsymbol{\mu}, \kappa) \text{ for } 1 \leq i \leq n\}.$$

We want to find maximum likelihood estimates for the parameters $\boldsymbol{\mu}$ and κ of the distribution $M_d(\boldsymbol{\mu}, \kappa)$. Assuming each $\mathbf{x}_i \in \mathcal{X}$ to be independent we can write the likelihood of $\mathcal{X}$ as:

$$P(\mathcal{X}|\boldsymbol{\mu}, \kappa) = P(\mathbf{x}_1, \ldots, \mathbf{x}_n|\boldsymbol{\mu}, \kappa) = \prod_{i=1}^{n} f(\mathbf{x}_i|\boldsymbol{\mu}, \kappa) = \prod_{i=1}^{n} c_d(\kappa) e^{\kappa \boldsymbol{\mu}^T \mathbf{x}_i}. \tag{2.3}$$

Taking logarithm of both sides of (2.3), the log-likelihood of the data set $\mathcal{X}$ becomes

$$\mathcal{L}(\mathcal{X}|\boldsymbol{\mu}, \kappa) = \ln P(\mathcal{X}|\boldsymbol{\mu}, \kappa) = n \ln c_d(\kappa) + \kappa \boldsymbol{\mu}^T \mathbf{r}, \tag{2.4}$$

where $\mathbf{r} = \sum_i \mathbf{x}_i$. To obtain the maximum likelihood parameter estimates of $\boldsymbol{\mu}$ and κ, we have to maximize (2.4), subject to the constraints $\boldsymbol{\mu}^T\boldsymbol{\mu} = 1$ and $\kappa \geq 0$. Introducing a Lagrange multiplier λ, the Lagrangian of the objective function is given by[2]

$$L(\boldsymbol{\mu}, \lambda, \kappa; \mathcal{X}) = n \ln c_d(\kappa) + \kappa\boldsymbol{\mu}^T\mathbf{r} + \lambda(1 - \boldsymbol{\mu}^T\boldsymbol{\mu}). \tag{2.5}$$

Now, taking derivatives of the Lagrangian with respect to $\boldsymbol{\mu}, \lambda$ and κ and setting them to zero, we get the following equations that the parameter estimates $\hat{\boldsymbol{\mu}}, \hat{\lambda}$ and $\hat{\kappa}$ must satisfy:

$$\hat{\boldsymbol{\mu}} = \frac{\hat{\kappa}}{2\hat{\lambda}}\mathbf{r}, \tag{2.6a}$$

$$\hat{\boldsymbol{\mu}}^T\hat{\boldsymbol{\mu}} = 1, \tag{2.6b}$$

$$\frac{nc_d'(\hat{\kappa})}{c_d(\hat{\kappa})} = -\hat{\boldsymbol{\mu}}^T\mathbf{r}. \tag{2.6c}$$

Substituting (2.6a) in (2.6b) gives us

$$\hat{\lambda} = \frac{\hat{\kappa}}{2}\|\mathbf{r}\|, \tag{2.7}$$

$$\hat{\boldsymbol{\mu}} = \frac{\mathbf{r}}{\|\mathbf{r}\|} = \frac{\sum_{i=1}^n \mathbf{x}_i}{\|\sum_{i=1}^n \mathbf{x}_i\|}, \quad \text{by } \; (2.6a). \tag{2.8}$$

Substituting (2.8) in (2.6c), we get

$$\frac{c_d'(\hat{\kappa})}{c_d(\hat{\kappa})} = -\frac{\|\mathbf{r}\|}{n}. \tag{2.9}$$

For brevity, let us write $s = d/2 - 1$; on differentiating (2.2) w.r.t. κ we obtain:

$$c_d'(\kappa) = \frac{s\kappa^{s-1}}{cI_s(\kappa)} - \frac{\kappa^s I_s'(\kappa)}{cI_s^2(\kappa)}, \tag{2.10}$$

where $c = (2\pi)^{s+1}$ is a constant. The right hand side simplifies to

$$\frac{\kappa^s}{cI_s(\kappa)}\left(\frac{s}{\kappa} - \frac{I_s'(\kappa)}{I_s(\kappa)}\right) = c_d(\kappa)\left(\frac{s}{\kappa} - \frac{I_s'(\kappa)}{I_s(\kappa)}\right). \tag{2.11}$$

Using the following well known recurrence relation ([AS74] 9.6.26)

$$\kappa I_{s+1}(\kappa) = \kappa I_s'(\kappa) - sI_s(\kappa), \tag{2.12}$$

we finally obtain:

$$\frac{-c_d'(\kappa)}{c_d(\kappa)} = \frac{I_{s+1}(\kappa)}{I_s(\kappa)} = \frac{I_{d/2}(\kappa)}{I_{d/2-1}(\kappa)}. \tag{2.13}$$

Thus we can obtain the m.l.e. $\hat{\kappa}$ by solving

$$A_d(\hat{\kappa}) = \frac{\|\mathbf{r}\|}{n}, \tag{2.14}$$

where $A_d(\kappa) = \frac{I_{d/2}(\kappa)}{I_{d/2-1}(\kappa)}$. In Section 4.2 we shall discuss the computation of $\hat{\kappa}$ from (2.14) using various approximations.

[2] strictly speaking, we should introduce the inequality constraint for κ in the Lagrangian and work with the necessary KKT conditions. If we assume κ cannot be 0, then the multiplier for the inequality constraint has to be zero by the complementary slackness conditions, and the Lagrangian we are working with is adequate.

3 EM on Mixture of vMFs

In this section, we introduce a mixture of k vMF (moVMF) distributions as a generative model for directional data. We then derive the mixture-density parameter estimation update equations from a given data set using the expectation maximization (EM) framework. The probability density function of the moVMF generative model is given by

$$f(\mathbf{x}|\Theta) = \sum_{h=1}^{k} \alpha_h f_h(\mathbf{x}|\theta_h), \tag{3.1}$$

where $\Theta = \{\alpha_1, \cdots, \alpha_k, \theta_1, \cdots, \theta_k\}$, $\alpha_h \geq 0$, $\sum_{h=1}^{k} \alpha_h = 1$ and $f_h(\mathbf{x}|\theta_h)$ is a single vMF distribution with parameters $\theta_h = (\boldsymbol{\mu}_h, \kappa_h)$. In order to sample a point from the generative model perspective, the h-th vMF is chosen at random with probability α_h, and then a point is sampled from $\mathbb{S}^{d-1}$ following $f_h(\mathbf{x}|\theta_h)$. Let $\mathcal{X} = \{\mathbf{x}_1, \cdots, \mathbf{x}_n\}$ be a data set generated by sampling independently following this generative model. Let $\mathcal{Z} = \{\mathrm{z}_1, \cdots, \mathrm{z}_n\}$ be the corresponding set of the so-called hidden random variables such that $\mathrm{z}_i = h$ when $\mathbf{x}_i$ has been generated following $f_h(\mathbf{x}|\theta_h)$. Then, with the knowledge of the values of the hidden variables, the log-likelihood of the observed data is given by

$$\ln P(\mathcal{X}, \mathcal{Z}|\Theta) = \sum_{i=1}^{n} \ln \left(\alpha_{\mathrm{z}_i} f_{\mathrm{z}_i}(\mathbf{x}_i|\theta_{\mathrm{z}_i})\right), \tag{3.2}$$

from which maximum likelihood parameter estimates can be obtained. However, the values of the hidden variables are not known, whereby (3.2) is really a random variable dependent on the distribution of $\mathcal{Z}$, and will be called the *complete data log-likelihood*. Now, for a given $(\mathcal{X}, \Theta)$, it is possible to obtain an estimate of the most likely conditional distribution of $\mathcal{Z}|(\mathcal{X}, \Theta)$, and this forms the E-step of the EM framework. The exact details of how this estimation is done will be deferred for the moment. In fact we will discuss two ways of estimating the hidden variable distributions that lead to significantly different algorithms. For now, we will assume that the distribution $p(h|\mathbf{x}_i, \Theta) = p(\mathrm{z}_i = h|\mathbf{x} = \mathbf{x}_i, \Theta), \forall h$, is known for all the data points.

3.1 The M-step: Parameter Estimation

Suppose the conditional distribution, $p(h|\mathbf{x}_i, \Theta), \forall h, i$, of the hidden variables $\mathcal{Z}|(\mathcal{X}, \Theta)$ is known. Unless otherwise specified, from this point onward, all expectations will taken over the distribution of the (set of) random variable(s) $\mathcal{Z}|(\mathcal{X}, \Theta)$. Now, expectation of the complete data log-likelihood given by (3.2), over the given distribution p, is given by

$$\begin{aligned} E_p[\ln P(\mathcal{X}, \mathcal{Z}|\Theta)] &= \sum_{i=1}^{n} E_{p(\mathrm{z}_i|\mathbf{x}_i,\Theta)}[\ln(\alpha_{\mathrm{z}_i} f_{\mathrm{z}_i}(\mathbf{x}_i|\theta_{\mathrm{z}_i}))] \\ &= \sum_{i=1}^{n} \sum_{h=1}^{k} \ln(\alpha_h f_h(\mathbf{x}_i|\theta_h))\ p(h|\mathbf{x}_i, \Theta) \\ &= \sum_{h=1}^{k} \sum_{i=1}^{n} (\ln \alpha_h)\ p(h|\mathbf{x}_i, \Theta) + \sum_{h=1}^{k} \sum_{i=1}^{n} (\ln f_h(\mathbf{x}_i|\theta_h))\ p(h|\mathbf{x}_i, \Theta). \end{aligned} \tag{3.3}$$

In the parameter estimation or M-step, Θ is re-estimated such that the above expression is maximized. Note that in order to maximize this expression, we can maximize the term containing α_h and the term containing θ_h separately since they are not related (note that $p(h|\mathbf{x}_i, \Theta)$ is fixed).

To find the expression for α_h, we introduce the Lagrangian multiplier λ with the constraint that $\sum_{h=1}^k \alpha_h = 1$ and take partial derivatives of the Lagrangian objective function w.r.t. each α_h to get

$$\frac{\partial}{\partial \alpha_h}\left[\sum_{h=1}^k \sum_{i=1}^n (\ln \alpha_h) p(h|\mathbf{x}_i, \Theta) + \lambda\left(\sum_{h=1}^k \alpha_h - 1\right)\right] = 0 \quad \Rightarrow \quad \sum_{i=1}^n p(h|\mathbf{x}_i, \Theta) = -\lambda \alpha_h, \quad \forall h. \tag{3.4}$$

Summing both sides of (3.4) over all h, we get $\lambda = -n$ and hence from (3.4) we have

$$\alpha_h = \frac{1}{n}\sum_{i=1}^n p(h|\mathbf{x}_i, \Theta). \tag{3.5}$$

Next we concentrate on the terms containing $\theta_h = (\boldsymbol{\mu}_h, \kappa_h)$ under the set of constraints $\boldsymbol{\mu}_h^T \boldsymbol{\mu}_h = 1, \kappa_h \geq 0, \forall h$. Then, using Lagrange multipliers $\lambda_1, \cdots, \lambda_k$ corresponding to these constraints, the Lagrangian is given by

$$\begin{aligned} L(\{\boldsymbol{\mu}_h, \lambda_h, \kappa_h\}_{h=1}^k) &= \sum_{h=1}^k \sum_{i=1}^n (\ln f_h(\mathbf{x}_i|\theta_h))\ p(h|\mathbf{x}_i, \Theta) + \sum_{h=1}^k \lambda_h\left(1 - \boldsymbol{\mu}_h^T \boldsymbol{\mu}_h\right) \\ &= \sum_{h=1}^k \left[\sum_{i=1}^n (\ln c_d(\kappa_h))\ p(h|\mathbf{x}_i, \Theta) + \sum_{i=1}^n \kappa_h \boldsymbol{\mu}_h^T \mathbf{x}_i\ p(h|\mathbf{x}_i, \Theta) + \lambda_h(1 - \boldsymbol{\mu}_h^T \boldsymbol{\mu}_h)\right]. \end{aligned} \tag{3.6}$$

Note that (3.6) is quite similar to the Lagrangian in (2.5) for a single vMF distribution. Now, taking partial derivatives of (3.6) with respect to $\{\boldsymbol{\mu}_h, \lambda_h, \kappa_h\}_{h=1}^k$ and setting them to zero, we get the following set of equations for $h = 1, 2, \ldots, k$:

$$\boldsymbol{\mu}_h = \frac{\kappa_h}{2\lambda_h}\sum_{i=1}^n \mathbf{x}_i p(h|\mathbf{x}_i, \Theta), \tag{3.7a}$$

$$\boldsymbol{\mu}_h^T \boldsymbol{\mu}_h = 1 \quad \forall h, \tag{3.7b}$$

$$\frac{c_d'(\kappa_h)}{c_d(\kappa_h)}\sum_{i=1}^n p(h|\mathbf{x}_i, \Theta) = -\boldsymbol{\mu}_h^T \sum_{i=1}^n \mathbf{x}_i p(h|\mathbf{x}_i, \Theta). \tag{3.7c}$$

As before, substituting (3.7a) in (3.7b), we get

$$\lambda_h = \frac{\kappa_h}{2}\left\|\sum_{i=1}^n \mathbf{x}_i p(h|\mathbf{x}_i, \Theta)\right\|, \tag{3.8}$$

$$\Rightarrow \boldsymbol{\mu}_h = \frac{\sum_{i=1}^n \mathbf{x}_i p(h|\mathbf{x}_i, \Theta)}{\|\sum_{i=1}^n \mathbf{x}_i p(h|\mathbf{x}_i, \Theta)\|}, \quad \text{by (3.7a).} \tag{3.9}$$

Finally, substituting (3.9) in (3.7c), we get

$$\frac{c_d'(\kappa_h)}{c_d(\kappa_h)} = -\frac{\|\sum_{i=1}^n \mathbf{x}_i p(h|\mathbf{x}_i, \Theta)\|}{\sum_{i=1}^n p(h|\mathbf{x}_i, \Theta)}, \tag{3.10}$$

which simplifies to

$$A_d(\kappa_h) = \frac{\|\sum_{i=1}^n \mathbf{x}_i p(h|\mathbf{x}_i, \Theta)\|}{\sum_{i=1}^n p(h|\mathbf{x}_i, \Theta)}, \tag{3.11}$$

where $A_d(\kappa) = \frac{I_{d/2}(\kappa)}{I_{d/2-1}(\kappa)}$. Note that (3.9) and (3.11) are intuitive generalizations of (2.8) and (2.14) respectively.

3.2 The E-step: Distribution estimation

From the standard setting of the EM algorithm [DLR77, Col97, Bil98], (3.5), (3.9), and (3.11) give the update equations of the parameters involved. Given this set of parameters, the distribution of the hidden variables can be computed [NH98, Bil98] as:

$$p(h|\mathbf{x}_i, \Theta) = \frac{\alpha_h \, f_h(\mathbf{x}_i|h, \Theta)}{\sum_{l=1}^{k} \alpha_l \, f_l(\mathbf{x}_i|l, \Theta)}. \tag{3.12}$$

It can be shown [Col97] that the *incomplete data log-likelihood*, $\ln p(\mathcal{X}|\Theta)$, is non-decreasing at each iteration of the parameter and distribution update. Iteration over this set of updates forms the basis of our algorithm `soft-moVMF` to be discussed in section 4.

Next, we discuss a nonstandard setting of the EM algorithm that is more practical for clustering algorithms. In this setting, points are *hard-assigned* to clusters so that effectively each of the hidden variables has a distribution that has probability 1 for one of the mixture components and zero for all the others. We shall denote this class of distributions as $\mathcal{H}$. Note that this does not follow naturally from the mixture model setting. However, we investigate this setting because of its computational efficiency and usability in practical clustering problems.

Consider the same mixture model setting, with the added constraint that the distributions of the hidden variables are restricted to $\mathcal{H}$. Note that $\mathcal{H}$ is a subset of all possible distributions on the events, and for a typical mixture model, the distribution following (3.12) will not belong to this subset. The important question is: is there a way to optimally pick a distribution from $\mathcal{H}$ and then perform a regular M-step, and guarantee that the incomplete log-likelihood of the data is non-decreasing at each iteration of the update? Unfortunately, this is not possible in general. However, we show that it is possible to reasonably lower bound the incomplete log-likelihood of the data using expectations over an *optimal* distribution $q \in \mathcal{H}$. The distribution $q \in \mathcal{H}$ is called optimal because it gives the tightest lower bound to the incomplete log-likelihood among all distributions in $\mathcal{H}$. The lower bound is reasonable in the sense that the expectation over q is itself lower bounded by (3.3), the expectation of the complete log-likelihood over the distribution p given by (3.12). Then, an iterative update scheme analogous to regular EM guarantees that the lower bound on the incomplete log-likelihood is non-decreasing at each iteration of the update. The parameter estimation, or, M-step remains practically unchanged, with p replaced by q in the update equations (3.5), (3.9), and (3.11). In the E-step, the optimal q is estimated. Thus, until a saddle-point is reached, this scheme does a greedy-optimal maximization of a lower bound on the incomplete log-likelihood of the data. This justifies the use of hard-assignment for learning mixture models and forms the basis of our algorithm `hard-moVMF` to be discussed in section 4.

At first, we state our hard assignment rule: if the optimal distribution in $\mathcal{H}$ is denoted by $q(h|\mathbf{x}_i, \Theta)$, then

$$q(h|\mathbf{x}_i, \Theta) = \begin{cases} 1, & \text{if } h = \underset{h'}{\operatorname{argmax}} \;\; p(h'|\mathbf{x}_i, \Theta), \\ 0, & \text{otherwise.} \end{cases} \tag{3.13}$$

We justify this hard assignment in two steps. First we show that the expectation over q is a reasonable lower bound of the incomplete log-likelihood of the data so that maximizing this expectation makes sense. Then, we show that the choice of this particular hard-assignment is the optimum in the sense that it gives the tightest lower bound among all distributions in $\mathcal{H}$.

At first, following the arguments in [NH98], we introduce the function $F(\tilde{p}, \Theta)$ given by

$$F(\tilde{p}, \Theta) = E_{\tilde{p}}[\ln P(\mathcal{X}, \mathcal{Z}|\Theta)] + H(\tilde{p}). \tag{3.14}$$

This function has the property that the E- and M-steps of the EM algorithm can be shown to *alternately maximize* this function. In the E-step, for a given value of Θ, the distribution $\tilde{p}$ is chosen to maximize $F(\tilde{p}, \Theta)$ for that Θ, and in the M-step, for a given value of $\tilde{p}$, the parameters Θ are estimated to maximize $F(\tilde{p}, \Theta)$ for the given $\tilde{p}$. It can be shown [NH98] that for a given Θ, the optimal $\tilde{p}$ is given by (3.12). When $\tilde{p} = p$, the optimal value of the function is given by

$$\begin{aligned} F(p, \Theta) &= E_p[\ln P(\mathcal{X}, \mathcal{Z}|\Theta)] + H(p) \\ &= E_p[\ln P(\mathcal{X}, \mathcal{Z}|\Theta)] - E_p[\ln P(\mathcal{Z}|(\mathcal{X}, \Theta))] \\ &= E_p\left[\ln\left(\frac{P(\mathcal{X}, \mathcal{Z}|\Theta)}{P(\mathcal{Z}|(\mathcal{X}, \Theta))}\right)\right] = E_p[\ln P(\mathcal{X}|\Theta)] \\ &= \ln P(\mathcal{X}|\Theta). \end{aligned} \tag{3.15}$$

Since (3.12) gives the optimal choice of the distribution, the functional value is smaller for any other choice of $\tilde{p}$. In particular, if $\tilde{p} = q$ as in (3.13), we have

$$F(q, \Theta) \leq F(p, \Theta) = \ln P(\mathcal{X}|\Theta). \tag{3.16}$$

Now, all distributions in $\mathcal{H}$ have the property that their entropy is 0. In particular, $H(q) = 0$. Then, from the definition of the function F, we have

$$E_q[\ln P(\mathcal{X}, \mathcal{Z}|\Theta)] \leq \ln P(\mathcal{X}|\Theta). \tag{3.17}$$

Thus, the expectation over q actually lower bounds the likelihood of the data. We go one step further to show that this is in fact a reasonably tight lower bound in the sense that the expectation over q is lower bounded by the expectation over p of the complete data log-likelihood. To this end, at first we prove the following result.

Lemma 1 $E_p[\ln P(\mathcal{Z}|(\mathcal{X}, \Theta))] \leq E_q[\ln P(\mathcal{Z}|(\mathcal{X}, \Theta))]$

Proof: Let $h_i^* = \underset{h}{\operatorname{argmax}}\, p(h|\mathbf{x}_i, \Theta)$. Then, $p(h|\mathbf{x}_i, \Theta) \leq p(h_i^*|\mathbf{x}_i, \Theta), \forall h$. Now, using the definitions of p and q, we have

$$\begin{aligned} E_p[\ln P(\mathcal{Z}|(\mathcal{X}, \Theta))] &= \sum_{i=1}^{n}\sum_{h=1}^{k} p(h|\mathbf{x}_i, \Theta) \ln p(h|\mathbf{x}_i, \Theta) \\ &\leq \sum_{i=1}^{n}\sum_{h=1}^{k} p(h|\mathbf{x}_i, \Theta) \ln p(h_i^*|\mathbf{x}_i, \Theta) \\ &= \sum_{i=1}^{n} \ln p(h_i^*|\mathbf{x}_i, \Theta) \sum_{h=1}^{k} p(h|\mathbf{x}_i, \Theta) \;=\; \sum_{i=1}^{n} \ln p(h_i^*|\mathbf{x}_i, \Theta) \\ &= \sum_{i=1}^{n}\sum_{h=1}^{k} q(h|\mathbf{x}_i, \Theta) \ln p(h|\mathbf{x}_i, \Theta) \\ &= E_q[\ln P(\mathcal{Z}|(\mathcal{X}, \Theta))]. \end{aligned}$$

That completes the proof. ■

Now, adding the incomplete data log-likelihood to both sides of the inequality in Lemma 1, we have

$$\begin{aligned} & E_p[\ln P(\mathcal{Z}|(\mathcal{X}, \Theta))] + \ln P(\mathcal{X}|\Theta) \leq E_q[\ln P(\mathcal{Z}|(\mathcal{X}, \Theta))] + \ln P(\mathcal{X}|\Theta) \\ \Rightarrow\quad & E_p[\ln(P(\mathcal{Z}|(\mathcal{X}, \Theta))P(\mathcal{X}|\Theta))] \leq E_q[\ln(P(\mathcal{Z}|(\mathcal{X}, \Theta))P(\mathcal{X}|\Theta))] \\ \Rightarrow\quad & E_p[\ln P(\mathcal{X}, \mathcal{Z}|\Theta)] \leq E_q[\ln P(\mathcal{X}, \mathcal{Z}|\Theta)]. \end{aligned} \tag{3.18}$$

From, (3.17) and (3.18), we have

$$E_{\mathcal{Z}|(\mathcal{X},\Theta)\sim p}[\ln P(\mathcal{X},\mathcal{Z}|\Theta)] \leq E_{\mathcal{Z}|(\mathcal{X},\Theta)\sim q}[\ln P(\mathcal{X},\mathcal{Z}|\Theta)] \leq \ln P(\mathcal{X}|\Theta). \tag{3.19}$$

Thus, the expectation over the hard-assignment distribution lies in between the incomplete data likelihood and the expectation over p of complete data likelihood and hence is a reasonable lower bound to the incomplete data likelihood value.

Finally, we show that our choice of the distribution q is optimal in the sense that the expectation over q gives the tightest lower bound among all distributions in $\mathcal{H}$. Let $\tilde{q}$ be any other distribution in the subset. Then,

$$\begin{aligned} E_{\tilde{q}}[\ln P(\mathcal{X},\mathcal{Z}|\Theta)] &= \sum_{i=1}^{n}\sum_{h=1}^{k}\tilde{q}(h|\mathbf{x}_i,\Theta)\ln p(h|\mathbf{x}_i,\Theta) \;=\; \sum_{i=1}^{n}\ln p(h_i|\mathbf{x}_i,\Theta) \\ &\leq \sum_{i=1}^{n}\ln p(h_i^*|\mathbf{x}_i,\Theta) \;=\; \sum_{i=1}^{n}\sum_{h=1}^{k} q(h|\mathbf{x}_i,\Theta)\ln p(h|\mathbf{x}_i,\Theta) \\ &= E_q[\ln P(\mathcal{X},\mathcal{Z}|\Theta)]. \end{aligned}$$

Hence, the choice of q as in (3.13) is optimal. This analysis forms the basis of our algorithm `hard-moVMF` to be discussed in section 4.

4 Algorithms

In this section, we propose two algorithms for clustering directional data based on the development in the previous section. These two algorithms are based on soft- and hard-assignment schemes [KMN97], and are respectively called `soft-moVMF` and `hard-moVMF`. The `soft-moVMF` algorithm, presented in Algorithm 1, estimates the parameters of the mixture model exactly following the derivations in section 3. Hence, it assigns soft (or probabilistic) labels to each point that are given by the posterior probabilities of the components of the mixture conditioned on the point. On termination, the algorithm gives the parameters $\Theta = \{\alpha_h, \boldsymbol{\mu}_h, \kappa_h\}_{h=1}^k$ of the k vMFs that model the data set $\mathcal{X}$, as well as the *soft-clustering*, i.e., the posterior probabilities $p(h|\mathbf{x}_i,\Theta), \forall h, i$. Appropriate convergence criteria determine when the algorithm should terminate.[3]

The `hard-moVMF` algorithm, presented in Algorithm 2 estimates the parameters of the mixture model by a hard assignment, or, *winner take all* strategy. In other words, we do the assignment of the points based on a derived posterior distribution given by (3.13). Thus, after the hard assignments in every iteration, each point *belongs* to a single cluster. As before, the updates of the component parameters are done using the posteriors of the components given the points. The only difference in this case is that the posterior probabilities can take only 0/1 values. On termination, the algorithm gives the parameters $\Theta = \{\alpha_h, \boldsymbol{\mu}_h, \kappa_h\}_{h=1}^k$ of the k vMFs that model the data set $\mathcal{X}$ under the hard assignment setup, and the *hard-clustering*, i.e., a disjoint k-partitioning of $\mathcal{X}$ based on the conditional posteriors q on the component vMF distributions.

4.1 Revisiting `spkmeans`

We briefly revisit the `spkmeans` algorithm [DM01] that has been shown to perform quite well for real life text clustering tasks [DM01, DFG01, BG02, BBM02]. We look at `spkmeans` in the

[3] Note that we can obtain a hybrid algorithm by combining the soft- and hard- approaches. In such an algorithm one would first perform some iterations that do soft assignments and later perform hard assignments. Further justification of this idea appears in section 8.

Algorithm 1 `soft-moVMF`

```
Input: Set $\mathcal{X}$ of data points on $\mathbb{S}^{d-1}$
Output: A soft clustering of $\mathcal{X}$ over a mixture of $k$ vMF distributions
  Initialize all $\alpha_h, \boldsymbol{\mu}_h, \kappa_h,\ h = 1, \cdots, k$
  repeat
    {The E (Expectation) step of EM}
    for $i = 1$ to $n$ do
      for $h = 1$ to $k$ do
        $p(\mathbf{x}_i|\theta_h) \leftarrow c_d(\kappa_h) e^{\kappa_h \boldsymbol{\mu}_h^T \mathbf{x}_i}$
        $p(h|\mathbf{x}_i, \Theta) \leftarrow \frac{\alpha_h p(\mathbf{x}_i|\theta_h)}{\sum_{h'=1}^{k} \alpha_{h'} p(\mathbf{x}_i|\theta_{h'})}$
      end for
    end for
    {The M (Maximization) step of EM}
    for $h = 1$ to $k$ do
      $\alpha_h \leftarrow \frac{1}{n} \sum_{i=1}^{n} p(h|\mathbf{x}_i, \Theta)$
      $\boldsymbol{\mu}_h \leftarrow \frac{\sum_{i=1}^{n} \mathbf{x}_i p(h|\mathbf{x}_i, \Theta)}{\| \sum_{i=1}^{n} \mathbf{x}_i p(h|\mathbf{x}_i, \Theta) \|}$
      $\kappa_h \leftarrow A_d^{-1} \left( \frac{\| \sum_{i=1}^{n} \mathbf{x}_i p(h|\mathbf{x}_i, \Theta) \|}{\sum_{i=1}^{n} p(h|\mathbf{x}_i, \Theta)} \right)$
    end for
  until *convergence criteria* are met
```

light of the developments in sections 3 and 4. Algorithm 3 outlines the `spkmeans` procedure. We observe that the `spkmeans` algorithm can be looked upon as a special case of `soft-moVMF` as well as of `hard-moVMF`, under certain restrictive assumptions on the generative model. More precisely, assume that the generative model of the mixture of vMFs is such that the priors of all the components are the same, i.e., $\alpha_h = 1/k, \forall h$. In order to get `spkmeans` as a special case of `soft-moVMF`, we further assume that all the components have (equal) infinite concentration parameters, i.e., $\kappa_h = \kappa \to \infty, \forall h$. With these assumptions, the E-step reduces to assigning a point to its *nearest* cluster where nearness is computed as a cosine similarity between the point and the cluster representative. Thus, a point $\mathbf{x}_i$ will be assigned to cluster $h^* = \underset{h}{\operatorname{argmax}}\ \mathbf{x}_i^T \boldsymbol{\mu}_h$, since

$$p(h^*|\mathbf{x}_i, \Theta) = \lim_{\kappa \to \infty} \frac{e^{\kappa\ \mathbf{x}_i^T \boldsymbol{\mu}_{h^*}}}{\sum_{h'=1}^{k} e^{\kappa\ \mathbf{x}_i^T \boldsymbol{\mu}_h}} \to 1, \tag{4.1}$$

and $p(h|\mathbf{x}_i, \Theta) \to 0, \forall h \neq h^*$ (assuming no ties).

In order show that `spkmeans` can also be seen as a special case of the `hard-moVMF` algorithm, in addition to assuming the priors of the components to be equal, we further assume that the concentration parameters of all the components are equal, i.e., $\kappa_h = \kappa, \forall h$. Then, `hard-moVMF` reduces to `spkmeans`. With these assumptions on the model, the estimation of the common concentration parameter is not needed since the hard assignment will depend only on the value of the cosine similarity $\mathbf{x}_i^T \boldsymbol{\mu}_h$. Given a set of values for $\{\boldsymbol{\mu}_h\}_{h=1}^k$, define $\mathcal{X}_h = \{\mathbf{x} : \mathbf{x} \in \mathcal{X}, h = \operatorname{argmax}_{h'}\ \mathbf{x}^T \boldsymbol{\mu}_{h'}\}$. It is easy to see that $\{\mathcal{X}_h\}_{h=1}^k$ forms a disjoint k-partitioning of $\mathcal{X}$. For a given set of values for $\{\boldsymbol{\mu}_h, \kappa_h\}_{h=1}^k$, we can rewrite the `hard-moVMF` algorithm using a similar notation of set partitions, $\mathcal{X}_h = \{\mathbf{x} : \mathbf{x} \in \mathcal{X}, h = \operatorname{argmax}_{h'}\ \kappa_{h'} \mathbf{x}^T \boldsymbol{\mu}_{h'}\}$.

Algorithm 2 `hard-moVMF`

```
Input: Set $\mathcal{X}$ of data points on $\mathbb{S}^{d-1}$
Output: A disjoint $k$-partitioning of $\mathcal{X}$
  Initialize all $\alpha_h, \boldsymbol{\mu}_h, \kappa_h,\ h = 1, \cdots, k$
  repeat
    {The E (Expectation) step of EM}
    for $i = 1$ to $n$ do
      for $h = 1$ to $k$ do
        $p(\mathbf{x}_i|\theta_h) \leftarrow c_d(\kappa_h) e^{\kappa_h \boldsymbol{\mu}_h^T \mathbf{x}_i}$
        $q(h|\mathbf{x}_i, \Theta) \leftarrow \begin{cases} 1, & \text{if } \ h = \underset{h'}{\arg\max}\ \alpha_{h'}\ p(\mathbf{x}_i|\theta_{h'}) \\ 0, & \text{otherwise.} \end{cases}$
      end for
    end for
    {The M (Maximization) step of EM}
    for $h = 1$ to $k$ do
      $\alpha_h \leftarrow \frac{1}{n} \sum_{i=1}^{n} q(h|\mathbf{x}_i, \Theta)$
      $\boldsymbol{\mu}_h \leftarrow \frac{\sum_{i=1}^{n} \mathbf{x}_i q(h|\mathbf{x}_i, \Theta)}{\| \sum_{i=1}^{n} \mathbf{x}_i q(h|\mathbf{x}_i, \Theta)\|}$
      $\kappa_h \leftarrow A_d^{-1} \left( \frac{\| \sum_{i=1}^{n} \mathbf{x}_i q(h|\mathbf{x}_i, \Theta)\|}{\sum_{i=1}^{n} q(h|\mathbf{x}_i, \Theta)} \right)$
    end for
  until convergence criteria are met
```

Algorithm 3 `spkmeans` [DM01]

```
Input: Set $\mathcal{X}$ of data points on $\mathbb{S}^{d-1}$
Output: A disjoint $k$-partitioning $\{\mathcal{X}_h\}_{h=1}^{k}$ of $\mathcal{X}$
  Initialize $\boldsymbol{\mu}_h,\ h = 1, \cdots, k$
  repeat
    {The E (Expectation) step of EM}
    Set $\mathcal{X}_h \leftarrow \phi,\ h = 1, \cdots, k$
    for $i = 1$ to $N$ do
      $\mathcal{X}_h \leftarrow \mathcal{X}_h \cup \{\mathbf{x}_i\}$ where $h = \underset{h'}{\text{argmax}}\ \mathbf{x}_i^T \boldsymbol{\mu}_{h'}$
    end for
    {The M (Maximization) step of EM}
    for $h = 1$ to $k$ do
      $\boldsymbol{\mu}_h \leftarrow \frac{\sum_{\mathbf{x} \in \mathcal{X}_h} \mathbf{x}}{\| \sum_{\mathbf{x} \in \mathcal{X}_h} \mathbf{x} \|}$
    end for
  until convergence criteria are met
```

4.2 Some Implementation issues

We infer from (2.14) that to calculate the m.l.e. for κ, we have to compute $A_d^{-1}(\bar{R})$. Since $A_d(\kappa)$ is a function that involves the ratio of Bessel Functions it is not possible to obtain a closed form functional inverse. Instead we resort to numerical or asymptotic methods. Using Appendix B we can show that for large κ, the m.l.e. $\hat{\kappa}$ is approximately $(d-1)/(2(1-\bar{R}))$. Similarly for small κ we obtain the approximation, $\tilde{\kappa} \approx d\bar{R}$. These estimates for $\tilde{\kappa}$ are not that good in practice, especially for high dimensional data. A better estimate (see Appendix B) is given by

$$\tilde{\kappa} = \frac{\bar{R}d - \bar{R}^3}{1 - \bar{R}^2}, \tag{4.2}$$

and this is the estimate that we use in our implementation.

5 Datasets

In this section we describe the datasets that we used for our experiments. We used data drawn from five sources: Simulation, Classic3, Yahoo News, CMU 20 Newsgroup and Yeast Gene Expressions.

- **Simulated Datasets:** We simulated mixtures of vMFs for testing the "quality" and correctness of our algorithms that were designed to work for moVMFs. We used a slight modification of the algorithm given in [Woo94] to generate a set of data points following a given vMF distribution. The algorithm is shown in Table 9 and was implemented in MATLAB. This algorithm allows us to sample data from a specified vMF distribution. We use this algorithm as a subroutine when simulating a Mixture of vMFs (see Table 8). Let the tuple (N, d, k) denote the number of sample points, the dimensionality of a sample point and the number of clusters respectively. We present two main simulated datasets in this article. The first dataset **small-mix** is just 2-dimensional and is used to illustrate soft-clustering. The second dataset **big-mix** is a high-dimensional dataset that could serve as a model for real world text datasets.

  1. **small-mix:** This dataset had $(N, d, k) = (50, 2, 2)$. The mean direction of each component was set to some random vector. For each component κ was set to 4. We present detailed results for this particular dataset later in this section.
  2. **big-mix:** This dataset had $(N, d, k) = (5000, 1000, 4)$. The mean direction of each component was set to some random vector, and κ for each component was also set to a random number of $O(d)$. The mixing weights for each component were: $(.251, .238, .252, .259)$.

- **Classic3 Datasets:** Classic3 is a well known collection of documents. Classic3 contains documents from three well-separated sources, so the clusters that are formed should be quite disjoint.

  1. **Classic3:** This dataset contains 3893 files, among which 1400 Cranfield documents are from aeronautical system papers, 1033 Medline documents are from medical journals, and 1460 Cisi documents are from information retrieval papers. The toolkit MC [DFG01] was used for creating the high-dimensional vector space model for the text documents and a total of 4666 words were used. Thus, each document, after normalization, is represented as a unit vector in a 4666 dimensional space. This is a relatively simple dataset in the sense that the documents in the 3 clusters are on completely different topics.

2. **Classic300:** Classic300 is a subset of 300 documents that we created from the original Classic3 dataset. This dataset has 100 documents from each of the three categories in Classic3. The dimensionality of the data was 5471.
3. **Classic400:** Classic400 is a subset of 400 documents that we created from the original Classic3 dataset. This dataset has 100 documents each from Medline and Cisi categories. The remaining 200 documents are from the Cran category. This dataset was specifically designed to create unbalanced clusters in an otherwise easily separable and balanced dataset. The dimensionality of the data was 6205.

- **Yahoo News dataset** K-series dataset is a collection of 2340 Yahoo news articles from 20 different categories. The underlying clusters in this dataset are highly skewed in terms of the number of documents per cluster, with sizes ranging from 9 to 494. The skewness presents some more challenges for clustering algorithms.

- **CMU Newsgroup datasets** The CMU Newsgroup dataset is a well known collection of documents. The original distribution is one that is mentioned in item 1 below. We considered not only the original dataset but some of its subsets.

  1. **The News20 dataset** is a collection of 19,997 messages, collected from 20 different USENET newsgroups. A 1000 messages from 19 newsgroups, and 997 from another were chosen at random and partitioned by newsgroup name. The headers for each of the messages were removed so that they do not bias the results. Using the toolkit MC, the high-dimensional model had a total of 25924 words. This is a typical text dataset that one may encounter in real life - it very high-dimensional, sparse and there is significant overlap between its clusters. In fact, some cross-posted articles appear multiple times in the dataset – once under every group in which they were posted. Another feature of this dataset is that the natural classes are perfectly balanced, i.e., the number of points in every class is the same.
  2. **Small CMU 20** is a collection of 2000 messages selected from the original News20 dataset. We selected 100 messages from each category in the original dataset. Hence this dataset has balanced classes (though there may be overlap). The dimensionality of the data was 13406.
  3. **Same 100/1000** is a collection of 100/1000 messages from 3 very similar newsgroups: comp.graphics, comp.os.ms-windows, comp.windows.x.
  4. **Similar 100/1000** is a collection of 100/1000 messages from 3 somewhat similar newsgroups: talk.politics.guns, talk.politics.mideast, talk.politics.misc.
  5. **Different 100/1000** is a collection of 100/1000 messages from 3 very different newsgroups: alt.atheism, rec.sport.baseball, sci.space.

- **Yeast Gene Expression dataset:** Gene expression data was selected to offer a different clustering domain. This domain brings with it the associated troubles of cluster validation because of the unavailability of true labels. Thus this dataset is a truer representative of a typical clustering scenario.

  Gene expression data is presented as a matrix of genes (rows) by expression values (columns). The expression vectors are constructed using DNA microarray experiments. We used a subset of the Rosetta Inpharmatics yeast gene expression set [HMJ$^+$00]. The original dataset consists of 300 experiments measuring expression of 6,048 yeast genes. Out of these we selected a subset of 996 genes for clustering. For each of the 996 genes the 300-element expression vector was normalized to have unit Euclidean (L_2) norm.

6 Experimental Results

In this section we compare the following four clustering algorithms on the datasets described in Section 5:

1. Spherical K-Means [DM01]—`spkmeans`,
2. Frequency Sensitive K-Means [BG02]—`fskmeans`,
3. moVMF based clustering using hard assignments (Section 3)—`hard-moVMF`,
4. moVMF based clustering using soft assignments (Section 3)—`soft-moVMF`.

Except the gene expression dataset, performance of the algorithms on all the datasets has been analyzed using *mutual information* between the cluster and class labels. Our algorithms were implemented in both C++ and MATLAB. Most of the results presented in this section are based on our C++ implementation. In all the experiments, all the algorithms were initialized with identical starting partitions to ensure a fair comparison. For all the artificial and text datasets, the correct underlying class labels of the data points are known. For a given clustering of the data, we construct the class-by-cluster confusion matrix and normalize it by the total number of documents under consideration. Now, a data point having class label c and cluster label h is an indicator of the joint occurrence of (c, h). For a large number of documents, the normalized confusion matrix approaches the expectation of this indicator by the law of large numbers. But since this expectation is exactly the probability of the joint event, in the limit of large data, the normalized confusion matrix gives the joint distribution of the class and cluster labels. The first measure we use for performance evaluation is the mutual information (MI) of this joint distribution. The MI gives the amount of statistical similarity between the class and cluster labels [CT91]. If X is a random variable for the cluster assignments and Y is a random variable for the pre-existing labels on the same data, then the mutual information is given by $I(X;Y) = E_{X,Y}[\ln \frac{p(X,Y)}{p(X)p(Y)}]$. Note that we have experimented with various normalizations of the MI (see, e.g., [SGM00, SG02]), but these normalizations hardly make any difference in terms of analysis and interpretability of the results. The Appendix shows all the plots with normalized values of mutual information.

6.1 Simulated data sets

This section presents the results obtained by running the experiments on data that was simulated to have been drawn from a mixture of vMF distributions. For a description of the data see Section 5.

6.1.1 Dataset small-mix

The **small-mix** dataset is a collection of fifty, two-dimensional points, drawn from a mixture of two vMF distributions. Figure 1 (a) shows a plot of the points. From the plot we observe that there are two clusters of points. Most points belong to either one cluster or the other. Some of the points seem to have mixed membership to each cluster. As we shall soon see, the soft-clustering algorithm identifies these points and assigns them fractionally to either cluster.

The clustering produced by our soft cluster assignment algorithm is shown in Figure 1 (b).

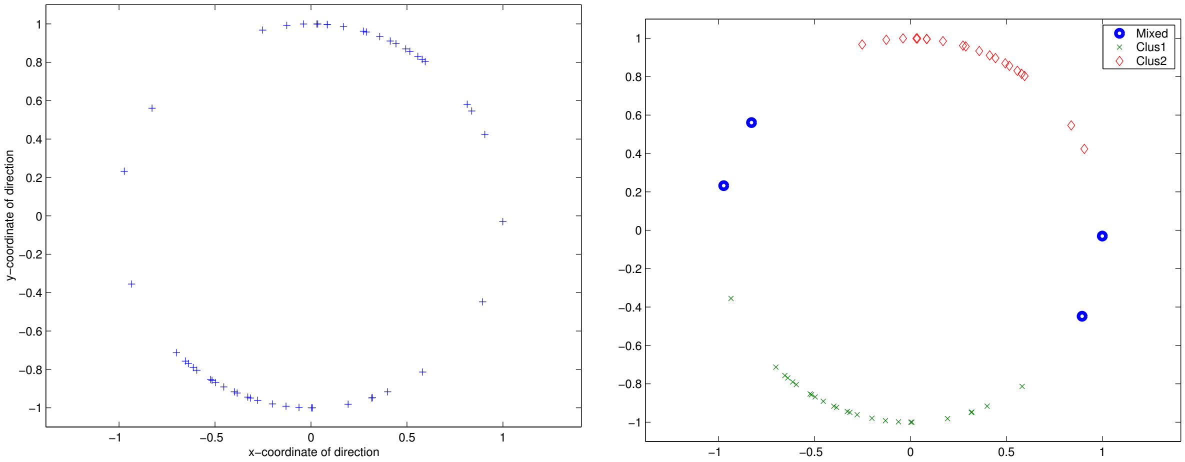

(a)
small-mix dataset

(b)
clustering of small-mix

Figure 1: Small-mix dataset and its clustering by `soft-moVMF`

In Figure 1(b), a point that has a probability ≥ 0.10, of membership to either cluster, is called a point with mixed membership. We see that the points that we would have visually assigned to both clusters, have been given a soft clustering.

The confusion matrix in Table 1 illustrates the clustering obtained by "hardening" the clustering produced by `soft-moVMF` for the small-mix dataset.

Class I	Class II
26	1
0	23

Table 1: Confusion matrix for clustering of small-mix by `soft-moVMF`

In Table 2 we compare the true and estimated parameters for the small-mix dataset estimated using `soft-moVMF`.

Cluster	$\boldsymbol{\mu}$	κ	$\hat{\boldsymbol{\mu}}$	$\hat{\kappa}$	$P(\omega)$	$\hat{P}(\omega)$
1	(-0.251, -0.968)	4	(-0.279, -0.960)	3.78	0.48	0.46
2	(0.399, 0.917)	4	(0.370, 0.929)	3.53	0.52	0.54

Table 2: True and estimated parameters for small-mix using `soft-moVMF`

In the table $\boldsymbol{\mu}, \kappa$ represent the true parameters and $\hat{\boldsymbol{\mu}}, \hat{\kappa}$ represent the estimated parameters. The true priors are given by $P(\omega)$ and the estimated priors are given by $\hat{P}(\omega)$. We can see the the estimated parameters quite closely approximate the true ones despite the small number of data points available.

6.1.2 Dataset big-mix

The second artificial dataset that we consider, more closely models what a real world text dataset could look like, with the exception that a real world text data set is usually more sparse. Figure 2 gives a plot of the MI of various algorithms that we used to cluster the data. Recall that the big-mix dataset was a set of 5000 points sampled from a mixture of four vMF distributions in 1000 dimensional space.

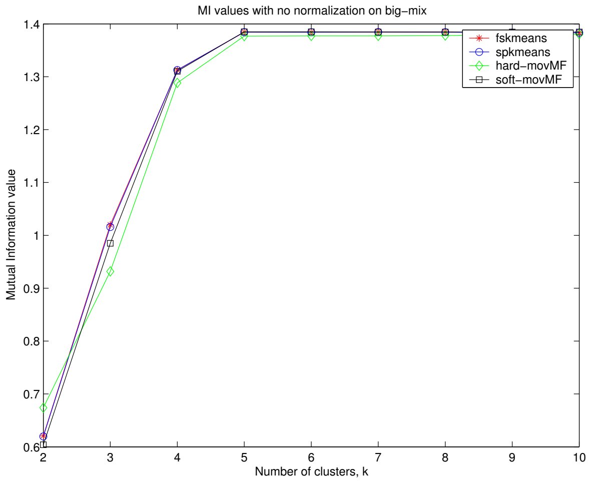

Figure 2: MI values for the big-mix dataset

From Figure 2 we observe that all the algorithms under consideration perform similarly and there is no discernible difference between their performance. We suspect that this absence of difference stems from the simplicity of the dataset as well the availability of a sufficient number of data points.

max $\boldsymbol{\mu}^T\hat{\boldsymbol{\mu}}$	avg $\boldsymbol{\mu}^T\hat{\boldsymbol{\mu}}$	max $\frac{\lvert\kappa-\hat{\kappa}\rvert}{\lvert\kappa\rvert}$	avg $\frac{\lvert\kappa-\hat{\kappa}\rvert}{\lvert\kappa\rvert}$	max $\frac{\lvert P(\omega)-\hat{P}(\omega)\rvert}{\lvert P(\omega)\rvert}$	avg $\frac{\lvert P(\omega)-\hat{P}(\omega)\rvert}{\lvert P(\omega)\rvert}$
0.999	0.998	0.006	0.004	0.002	0.001

Table 3: Performance of `soft-moVMF` on big-mix dataset

6.2 The Classic3 family of datasets

We now discuss the performance of the algorithms on the Classic3 family of datasets. First we present typical confusion matrices generated by the various algorithms on these datasets for the correct number of clusters.

Table 4 shows the confusion matrices obtained on the full Classic3 dataset. As can be easily seen from these confusion matrices, the performance of all the algorithms is quite similar. It seems for the full Classic3 dataset there is no added advantage yielded by using the general moVMF model as compared to the other algorithms. This observation can be explained by noting that the full Classic3 has a sufficient number of documents per cluster and each cluster is well separated from the other clusters. Thus, when finding clusters that equal the number of true clusters, the task is not very difficult.

fskmeans			spkmeans			hard-moVMF			soft-moVMF		
cisi	med	cran	cisi	med	cran	cisi	med	cran	cisi	med	cran
1019	0	0	1019	0	0	1018	0	0	1	4	1384
1	6	1386	1	6	1386	2	6	1387	13	1456	13
13	1454	12	13	1454	12	13	1454	11	1019	0	1

Table 4: Comparative confusion matrices for 3 clusters of Classic3.

Table 5 shows the confusion matrices obtained on the Classic300 dataset. Even though the dataset is separable, the low number of documents per cluster makes the problem somewhat difficult for fskmeans and spkmeans, while hard-moVMF has a much better performance due to its model flexibility. The soft-moVMF algorithm performs appreciably better than the other three algorithms. It seems that the low number of documents does not pose a problem for soft-moVMF and it ends up getting an almost perfect clustering for this dataset. Thus in this case, despite the low number of points per cluster, the superior modeling power of our moVMF based algorithms prevents them from getting trapped in inferior local-minima as compared to the other algorithms resulting in a better clustering.

fskmeans			spkmeans			hard-moVMF			soft-moVMF		
cisi	med	cran	cisi	med	cran	cisi	med	cran	cisi	med	cran
29	38	22	29	38	22	3	72	1	0	98	0
31	27	38	31	27	38	62	28	17	1	0	100
40	35	40	40	35	40	35	0	82	99	2	0

Table 5: Comparative confusion matrices for 3 clusters of Classic300.

The confusion matrices obtained on the Classic400 dataset are shown in Table 6. The behavior of the algorithms on this dataset is very interesting. As before, due to the small number of documents per cluster, fskmeans and spkmeans give a rather mixed confusion matrix. The hard-moVMF algorithm gets a significant part of the bigger cluster correctly and achieves some amount of separation between the two smaller clusters. The soft-moVMF algorithm exhibits the most interesting behavior. It splits the bigger cluster into two, quite pure segments, and merges the smaller two into one cluster. When 4 clusters are requested from soft-moVMF, it returns 4 very pure clusters (not shown in the confusion matrix) two of which are almost equal sized segments of the bigger cluster.

fskmeans			spkmeans			hard-moVMF			soft-moVMF		
cisi	med	cran	cisi	med	cran	cisi	med	cran	cisi	med	cran
27	16	55	27	17	54	56	28	20	0	0	91
51	83	12	51	82	12	44	72	14	82	99	2
23	1	132	23	1	133	1	0	165	19	1	106

Table 6: Comparative confusion matrices for 3 clusters of Classic400.

Another interesting insight into the behavior of the algorithms is obtained by considering their clustering performance when they are requested to produce more than the natural number of clusters for a given dataset. In Table 7 we present the confusion matrices when 5 clusters were produced for the main Classic3 dataset. It seems that the moVMF algorithms have a tendency of trying to maintain the larger clusters intact as long as possible, and breaking them into reasonably pure and equal parts when they are forced to do so. This behavior and the observation in Table 6 suggests that in practice one could generate a slightly higher number of clusters than required, and then agglomerate them appropriately.

fskmeans			spkmeans			hard-moVMF			soft-moVMF		
cisi	med	cran	cisi	med	cran	cisi	med	cran	cisi	med	cran
2	4	312	2	4	323	3	5	292	0	1	1107
8	520	10	8	512	9	511	1	0	5	1455	14
5	936	6	5	944	6	514	1	0	526	2	1
1018	0	1	1018	0	1	0	2	1093	501	0	0
0	0	1069	0	0	1059	5	1451	13	1	2	276

Table 7: Comparative confusion matrices for 5 clusters of Classic3.

Next we look at the MI plots for the various Classic3 datasets (Figures 3(a)-(c)). In the full Classic3 dataset (Figure 3(a)), all the algorithms perform almost similarly at the true number of clusters. However, as the number of clusters increases, soft-moVMF seems to outperform the others by a significant margin. Another interesting point to note is that the MI values from the hard-moVMF algorithm fall very rapidly beyond the true number of clusters—this particular behavior could be used as a guideline to automatically figure out the "true" number of clusters for a dataset where such a number is unknown (e.g. gene data). In the classic300 (Figure 3(b)) and the classic400 (Figure 3(c)) datasets, soft-moVMF seems to appreciably outperform the other algorithms. In fact, for these two datasets, soft-moVMF performs significantly better than the other three even at the correct number of clusters. Among the other three, hard-moVMF seems to perform better than spkmeans and fskmeans consistently over the entire range of values for the number of clusters over which experiments were run.

6.3 Yahoo News dataset

For the Yahoo News dataset, since the number of natural clusters is 20, we do not present samples of the confusion matrix obtained from the various clustering algorithms. Instead, we straightaway present the MI plots for the different algorithms for various number of clusters in Figure 3(d). An immediately observable fact is that soft-moVMF consistently performs better than the other algorithms. Even at the correct number of clusters, it performs significantly better than the other algorithms. As in the classic3 dataset, hard-moVMF again peaks at the true number of clusters, and then rapidly falls down with an increasing number of clusters. Among the other two, spkmeans performs better than fskmeans especially for higher values of the number of clusters. Since fskmeans has an explicit mechanism for trying to form clusters of approximately equal size, and since the natural clusters in the yahoo20 dataset are heavily skewed, fskmeans suffers due to its bias. On the other hand spkmeans does not have any such bias and hence does reasonably well even for a high number of clusters.

6.4 CMU Newsgroup family of datasets

We now turn our attention to the performance of the algorithms on the News20 datasets. Figure 4(a) shows the MI plots on the full cmu-1000 dataset. All the algorithms perform similarly till the true number of clusters after which soft-moVMF and spkmeans perform better than the others. The results for the cmu-100 (Figure 4(b)) dataset are of course different. Since the number of documents per cluster is small, as before spkmeans and fskmeans do not perform that well, even at the true number of clusters, whereas soft-moVMF performs significantly better than the others over

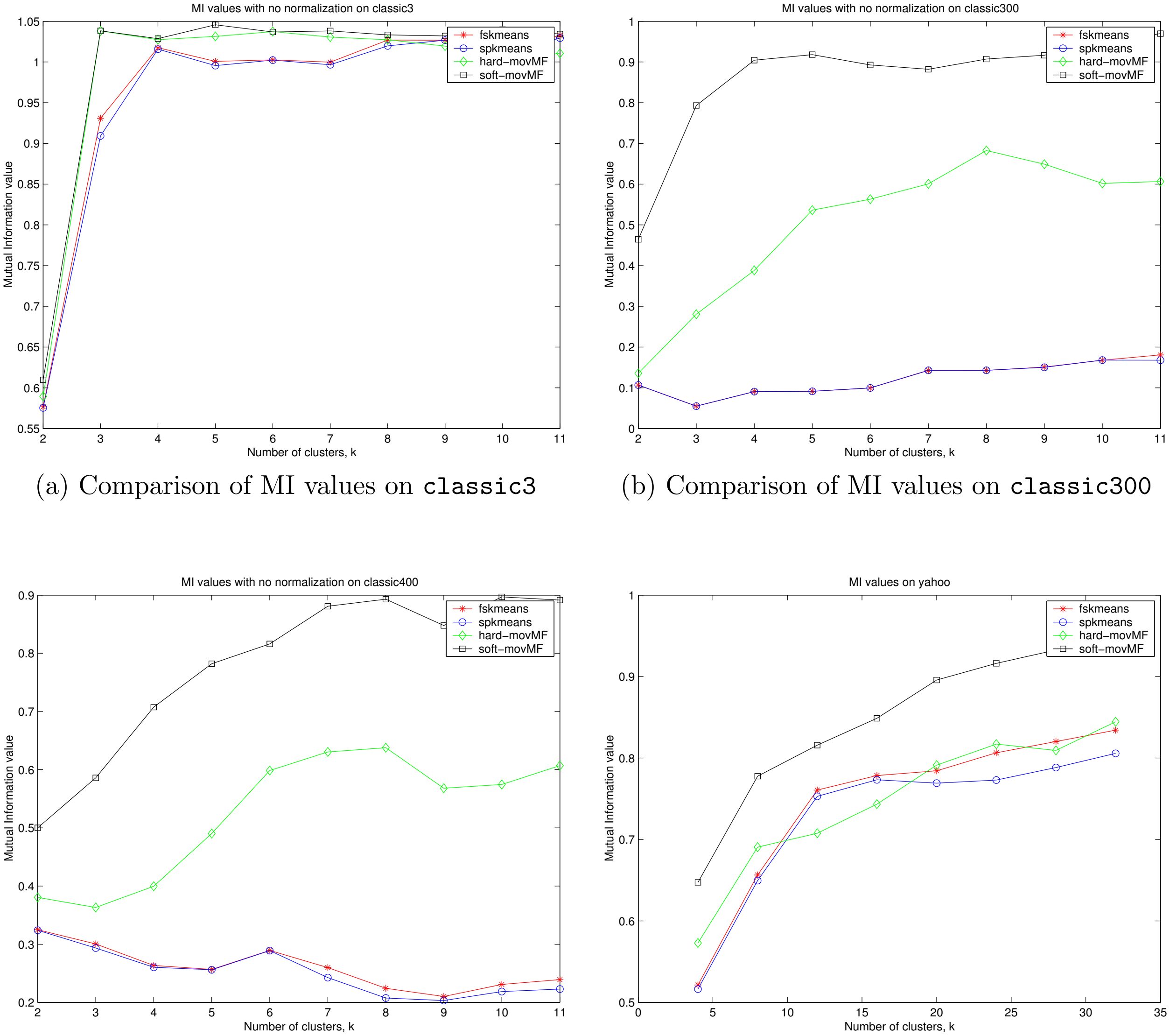

(a) Comparison of MI values on `classic3`

(b) Comparison of MI values on `classic300`

(c) Comparison of MI values on `classic400`

(d) Comparison of MI values on `yahoo20`

Figure 3: Comparison of the algorithms on the Classic3 datasets and the Yahoo News dataset

the entire range. Again, `hard-moVMF` gives good MI values till the true number of clusters after which it falls sharply. In fact, this behavior is repeatedly observed in all the datasets having small number of documents per cluster — `different-100` (Figure 4(c)), `similar-100` (Figure 5(a)), and `same-100`(Figure 5(c)). On the other hand, for the datasets having a reasonably large number of documents per cluster, another kind of behavior is observed. All the algorithms perform quite similarly till the true number of clusters, after which `soft-moVMF` performs significantly better than the other three. This behavior can be observed in Figures 4(d), 5(b) and 5(d). We note that the other three algorithms perform quite similarly over the entire range. A closer look reveals that `hard-moVMF` maintains its previously observed behavior of sharply rising at the true number of clusters and then falling sharply for higher values of the number of clusters. In fact, it achieves the highest MI value among all the algorithms at the true number of clusters for `similar-1000` and `same-1000`.

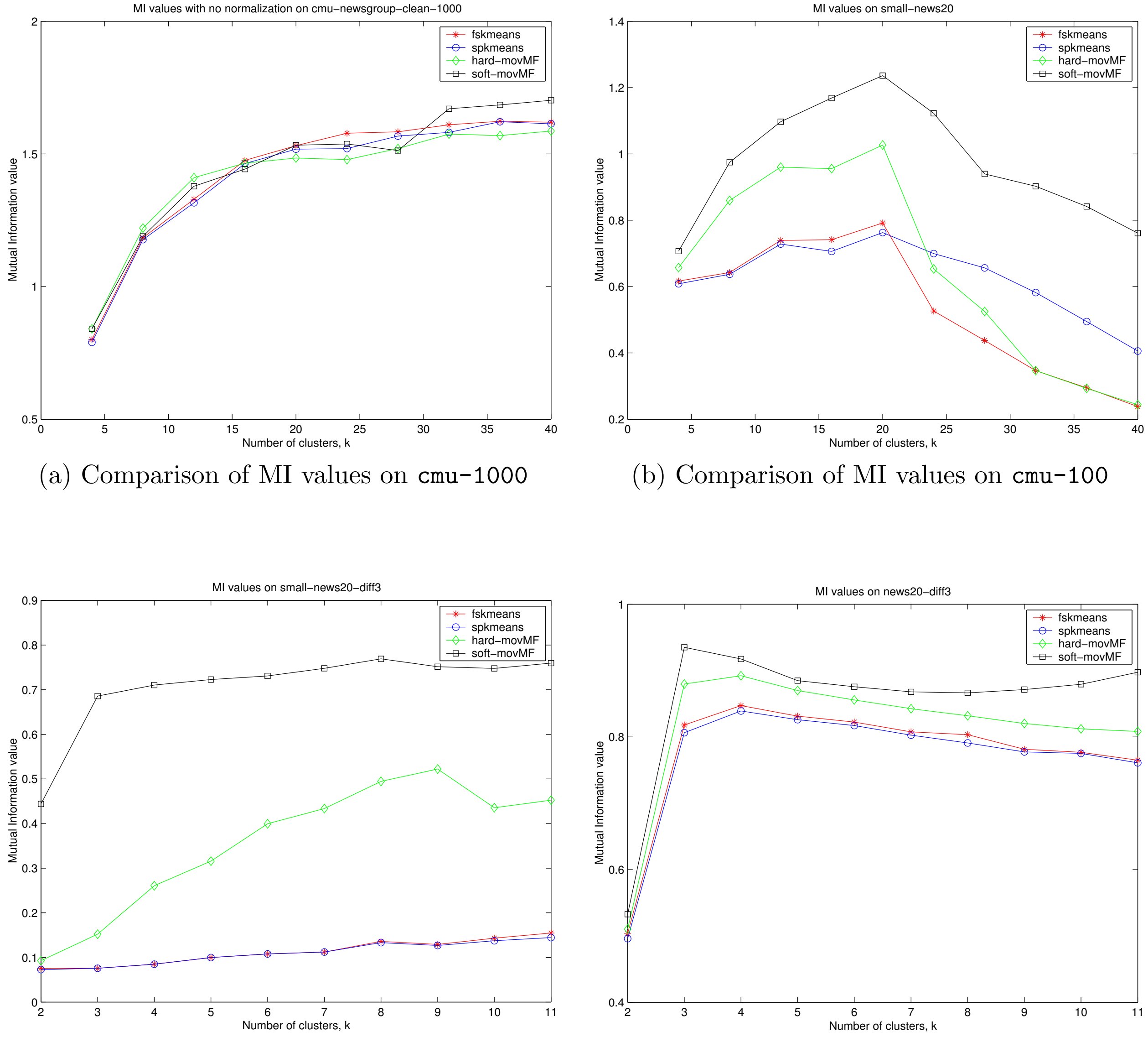

(a) Comparison of MI values on `cmu-1000`

(b) Comparison of MI values on `cmu-100`

(c) Comparison of MI values on `different-100`

(d) Comparison of MI values on `different-1000`

Figure 4: Comparison on the various versions of the News20 datasets

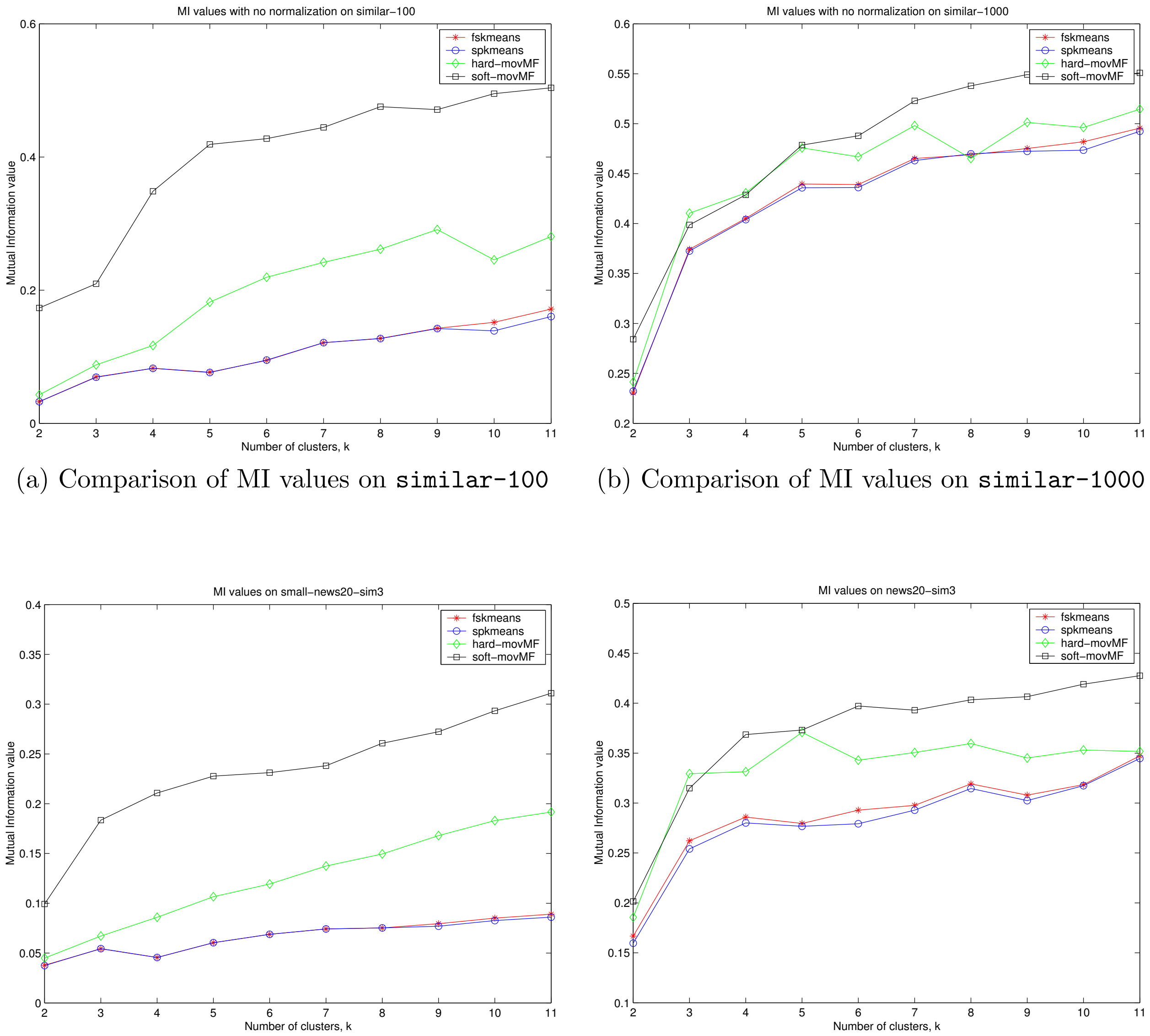

(a) Comparison of MI values on `similar-100`

(b) Comparison of MI values on `similar-1000`

(c) Comparison of MI values on `same-100`

(d) Comparison of MI values on `same-1000`

Figure 5: Comparison on the various versions of the News20 dataset

6.5 Gene expression data

We now move onto a domain different from text clustering, viz., clustering of gene expression data. We consider a yeast gene dataset as described in section 5. The dataset considered has two main differences as compared to text data, firstly the data can have negative values and secondly we do not know the true labels for the data points. Since true labels for the genes are not known,[4], we have to resort to other validation procedures to evaluate the clustering obtained.

6.5.1 Validation method

We compute some traditional figures of merit [SS00] to evaluate the quality of clustering obtained by each algorithm. Let $\mathcal{X} = \{\mathbf{x}_1, \mathbf{x}_2, \ldots \mathbf{x}_n\}$ be the set of data that is clustered. Let $\mu(\mathbf{x})$ denote the mean vector of the cluster to which $\mathbf{x}$ belongs. The homogeneity of the clustering is measured by:

$$H_{avg} = \frac{1}{|\mathcal{X}|} \sum_{\mathbf{x} \in \mathcal{X}} \frac{\mathbf{x}^T \mu(\mathbf{x})}{\|\mathbf{x}^T\| \|\mu(\mathbf{x})\|}. \tag{6.1}$$

As can easily be seen, a higher homogeneity means that the individual elements of each cluster are quite similar to the cluster representative. We also take note of the minimum similarity

$$H_{min} = \min_{\mathbf{x} \in \mathcal{X}} \frac{\mathbf{x}^T \mu(\mathbf{x})}{\|\mathbf{x}^T\| \|\mu(\mathbf{x})\|}. \tag{6.2}$$

Both H_{avg} and H_{min} provide a measure of the intra-cluster similarity. We now define the inter cluster separation as follows:

$$S_{avg} = \frac{1}{\sum_{i \neq j} |C_i||C_j|} \sum_{i \neq j} |C_i||C_j| \frac{\boldsymbol{\mu}_i^T \boldsymbol{\mu}_j}{\|\boldsymbol{\mu}_i\| \|\boldsymbol{\mu}_j\|}, \tag{6.3}$$

where $|C_i|$ and $\boldsymbol{\mu}_i$ represent the size and mean of cluster i, respectively. We also measure the maximum inter-cluster similarity as:

$$S_{max} = \max_{i \neq j} \frac{\boldsymbol{\mu}_i^T \boldsymbol{\mu}_j}{\|\boldsymbol{\mu}_i\| \|\boldsymbol{\mu}_j\|}. \tag{6.4}$$

It is easily seen that for a “good” clustering S_{avg} and S_{max} should be low.

6.5.2 Results

Figure 6 shows the various cluster quality figures of merit as described in the previous section for our gene expression dataset. The first fact that one observes is that `hard-moVMF` consistently performs better than all the other algorithms. This comes as a little bit of a surprise, because in almost all other datasets, `soft-moVMF` performed better (though, of course, the measures of evaluation are different for gene data as compared to the other datasets that we considered). Note that the figures of merit were computed for `soft-moVMF` by “hardening” the clustering results that it produced.

[4] In fact we believe that many genes would ideally have multiple labels, because each gene might be responsible for more than one function in the cell. Thus ideally we want to know the “true” soft labels. The aim of the soft clustering algorithm is to try and obtain such labels for each gene.

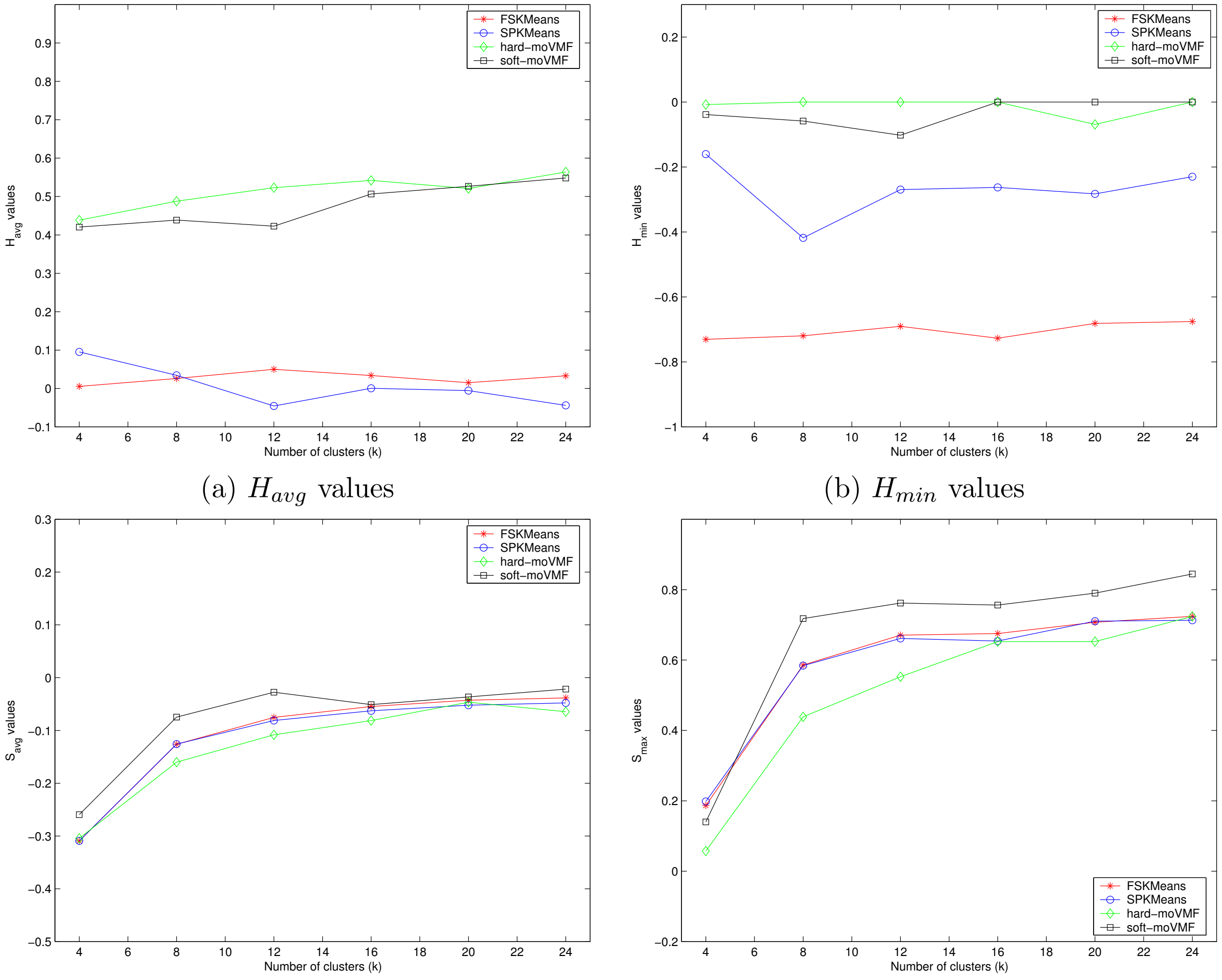

(a) H_{avg} values

(b) H_{min} values

(c) S_{avg} values

(d) S_{max} values

Figure 6: Measures of cluster quality for gene data

We see from Figure 6(a) that both `hard-moVMF` and `soft-moVMF` yield clusters that are much more homogeneous than those yielded by `fskmeans` and `spkmeans`. The inter-cluster similarities, as measured by S_{avg} and S_{max} are again the lowest for `hard-moVMF`, thereby indicating that `hard-moVMF` gives the best separated clusters of all the four algorithms. We note, however, that the inter-cluster similarities do not differ that much between the four algorithms but `soft-moVMF` seems to be forming clusters with higher inter-cluster similarity than other algorithms. We can explain this behavior of `soft-moVMF` by noting that it tends to form overlapping clusters (because of soft-assignments) and those clusters remain closer even after hardening. Since H_{avg} essentially measures the average cosine similarity, we note that using our moVMF based algorithms, we are able to achieve clusters that are more coherent and better separated—a fact that could be attributed to the richer model employed by our algorithms.

7 Limitations

Various problems arise for text data, or in-fact any other high-dimensional data when trying to model them using an exponential family based probability distribution. One salient feature of text data is that all features are necessarily non-negative. As a result, all the data-points lie on the surface of the first orthant of the d-dimensional hypersphere. Now, the surface area of the first orthant is just $1/2^d$ times the total surface area, and since all the data is present in this orthant, the concentration of the data increases exponentially (we observe $\kappa \propto d$). Hence, the concentration parameters κ of all the vMF distributions effectively go up at a similar rate with the dimensionality. Since the posterior probabilities of a cluster given a data point for the mixture of vMF models, or any mixture of exponential models for that matter, essentially follow a Gibbs distribution, and since high κ acts as a multiplier in the exponent, it can be seen that the posterior probabilities go to either 1 or 0. Hence, for very high-dimensions, the soft assignment case effectively boils down to the hard assignment case and no "soft" posterior probability values are obtained. Note, however, during the first few iterations of the `soft-moVMF` algorithm the probability values are of different from 0 and 1—an outcome of our initialization of κ to a small value.

8 Conclusions and Future Work

In this article we have proposed two algorithms for clustering directional data. The algorithms are essentially expectation maximization schemes on an appropriate generative model, namely a mixture of von Mises-Fisher distributions. High-dimensional text data after L_2 normalization has properties that match well with the requirements/assumptions of the vMF mixture model, and hence the proposed algorithms are powerful clustering techniques for text data. In fact, we showed that the `spkmeans` algorithm [DM01], that has been shown to work well for text clustering, is a special case of both of our proposed schemes. Another text clustering algorithm, `fskmeans` [BG02], is just a variant of the same special case. All the algorithms are comprehensively evaluated using both artificial and real life high dimensional data clustering tasks of varying degrees of complexity. The analysis and experiments show that expectation maximization schemes on mixtures of vMF distributions under various assumptions form a class of powerful clustering algorithms for directional data. This, together with the observation that a lot of high-dimensional sparse data can actually be modeled as directional data under appropriate normalization, demonstrates the usefulness of the proposed techniques.

The vMF distribution that we considered in the proposed techniques, is one of the simplest parametric distributions for directional data. More general models, e.g., the Fisher-Bingham distribution [MJ00], have more expressive power and may be useful under certain circumstances. However, the parameter estimation problem will be significantly more difficult for such models. Also, one would need a lot of data to get reliable estimates of the parameters. Hence the general models may not be a feasible option for most problems. Nevertheless, the tradeoff between model complexity and computational complexity needs to be studied properly to get a better understanding of model selection for directional data used for clustering.

Further work would be to look at more domains where data can be profitably modeled as a mixture of vMF distributions. The results that we observed for gene expression data were quite interesting. Our moVMF based algorithms gave clusters that were much more coherent (homogeneous) than the ones give by `fskmeans` and `spkmeans`. A closer investigation of the performance of our algorithms is needed to gain a better understanding of their behavior.

References

[AS74] M. Abramowitz and I. A. Stegun, editors. *Handbook of Mathematical Functions.* Dover Publ. Inc., New York, 1974.

[BBM02] S. Basu, A. Banerjee, and R. Mooney. Semi-supervised clustering by seeding. In *Proceedings International Conference on Machine Learning*, 2002.

[BG02] A. Banerjee and J. Ghosh. Frequency sensitive competitive learning for clustering on high-dimensional hyperspheres. In *Proceedings International Joint Conference on Neural Networks*, pages 1590–1595, May 2002.

[Bil98] J. A. Bilmes. A gentle tutorial of the EM algorithm and its application to parameter estimation for gaussian mixture and hidden markov models. Technical report, U. C. Berkeley, April 1998.

[Col97] M. Collins. The EM algorithm. In fulfillment of Written Preliminary Exam II requirement, September 1997.

[CT91] T. M. Cover and J. A. Thomas. *Elements of Information Theory.* Wiley-Interscience, 1991.

[DFG01] I. S. Dhillon, J. Fan, and Y. Guan. Efficient clustering of very large document collections. In V. Kumar R. Grossman, C. Kamath and R. Namburu, editors, *Data Mining for Scientific and Engineering Applications.* Kluwer Academic Publishers, 2001.

[DHS00] R. O. Duda, P. E. Hart, and D. G. Stork. *Pattern Classification.* John Wiley & Sons, 2000.

[DLR77] A. P. Dempster, N. M. Laird, and D. B. Rubin. Maximum likelihood from incomplete data via the EM algorithm. *Journal of the Royal Statistical Society, Series B*, 39:1–38, 1977.

[DM01] I. S. Dhillon and D. S. Modha. Concept decompositions for large sparse text data using clustering. *Machine Learning*, 42(1):143–175, 2001.

[DS03] I. S. Dhillon and S. Sra. Modeling data using directional distributions. Technical Report TR-03-06, University of Texas at Austin, Austin, TX, 2003.

[ESBB98] M. B. Eisen, P. T. Spellman, P. O. Brown, and D. Botstein. Cluster analysis and display of genome-wide expression patterns. *Proc. Natl. Acad. Sci.*, 95:14863–14868, 1998.

[FBY92] W. B. Frakes and R. Baeza-Yates. *Information Retrieval: Data Structures and Algorithms.* Prentice Hall, 1992.

[Gho03] J. Ghosh. Scalable clustering methods for data mining. In Nong Ye, editor, *Handbook of Data Mining*, pages 247–277. Lawrence Erlbaum, 2003.

[Hil81] G. W. Hill. Evaluation and inversion of the ratios of modified bessel functions. *ACM Transactions on Mathematical Software*, 7(2):199–208, June 1981.

[HMJ$^+$00] T. R. Hughes, M. J. Marton, A. R. Jones, C. J. Roberts, R. Stoughton, C. D. Armour, H. A. Bennett, E. Coffey, H. Dai, D. D. Shoemaker, D. Gachotte, K. Chakraburtty, J. Simon, M. Bard, and S. H. Friend. Functional discovery via a compendium of expression profiles. *Cell*, 102:109–126, 2000.

[Ind99] P. Indyk. A sublinear-time approximation scheme for clustering in metric spaces. In *40th Symposium on Foundations of Computer Science*, 1999.

[JD88] A. K. Jain and R. C. Dubes. *Algorithms for Clustering Data.* Prentice Hall, New Jersey, 1988.

[JH99] T. Jaakkola and D. Haussler. Exploiting generative models in discriminative classifiers. In M. S. Kearns, S. A. Solla, and D. D. Cohn, editors, *Advances in Neural Information Processing Systems*, volume 11, pages 487–493. MIT Press, 1999.

[KMN97] M. Kearns, Y. Mansour, and A. Ng. An information-theoretic analysis of hard and soft assignment methods for clustering. In *13th Annual Conf. on Uncertainty in Artificial Intelligence (UAI97)*, 1997.

[LRM$^+$97] D. A. Lashkari, J. L. De Risi, J. H. McCusker, A. F. Namath, C. Gentile, S. Y. Hwang, P. O. Brown, and R. W. Davis. Yeast microarrays for genome wide parallel genetic and gene expression analysis. *Proc. Natl. Acad. Sci.*, 94:13057–13062, 1997.

[Mac67] J. MacQueen. Some methods for classification and analysis of multivariate observations. In *Proc. 5th Berkeley Symp. Math. Statist. Prob.*, volume 1, pages 281–297, 1967.

[Mar75] K. V. Mardia. *Statistical Distributions in Scienctific Work*, volume 3, chapter Characteristics of directional distributions, pages 365–385. Reidel, Dordrecht, 1975.

[MJ00] K. V. Mardia and P. Jupp. *Directional Statistics.* John Wiley and Sons Ltd., 2nd edition, 2000.

[MPT$^+$99] E. M. Marcotte, M. Pellegrini, M. J. Thompson, T. Yeates, and D. Eisenberg. A combined algorithm for genome-wide prediction of protein function. *Nature*, 402:83–86, 1999.

[NH98] R. M. Neal and G. E. Hinton. A view of the EM algorithm that justifies incremental, sparse, and other variants. In M. I. Jordan, editor, *Learning in Graphical Models*, pages 355–368. MIT Press, 1998.

[Rao73] C. R. Rao. *Linear Statistical Inference and its Applications.* Wiley, New York, 2nd edition, 1973.

[Ros98] K. Rose. Deterministic annealing for clustering, compression, classification, regression, and related optimization problems. *Proc. IEEE*, 86(11):2210–39, 1998.

[Sal89] Gerard Salton. *Automatic text processing: the transformation, analysis, and retrieval of information by computer.* Addison-Wesley (Reading MA), 1989.

[SG02] A. Strehl and J. Ghosh. Cluster ensembles - a knowledge reuse framework for combining multiple partitions. *Journal of Machine Learning Research (in review)*, 2002.

[SGM00] A. Strehl, J. Ghosh, and R. Mooney. Impact of similarity measures on web-page clustering. In *Proc 7th Natl Conf on Artificial Intelligence : Workshop of AI for Web Search (AAAI 2000)*, pages 58–64. AAAI, July 2000.

[SKKR01] B. M. Sarwar, G. Karypis, J. A. Konstan, and J. Reidl. Item-based collaborative filtering recommendation algorithms. In *World Wide Web*, 10, pages 285–295, 2001.

[Smy97] P. Smyth. Clustering sequences with hidden Markov models. In M. C. Mozer, M. I. Jordan, and T. Petsche, editors, *Advances in Neural Information Processing*, volume 9, pages 648–654. MIT Press, 1997.

[SS00] R. Sharan and R. Shamir. CLICK: A clustering algorithm with applications to gene expression analysis. In *Proceedings of 8th International Conference on Intelligent Systems for Molecular Biology (ISMB)*, pages 307–316. AAAI Press, 2000.

[SS01] B. Schölkopf and A. Smola. *Learning with Kernels.* MIT Press, 2001.

[Vap98] V. N. Vapnik. *Statistical Learning Theory.* Wiley-Interscience, 1998.

[Wat96] G. N. Watson. *A treatise on the theory of Bessel functions.* Cambridge Mathematical Library. Cambridge University Press, 2nd (1944) edition, 1996.

[Woo94] A. T. A. Wood. Simulation of the von-Mises Distribution. *Communications of Statistics, Simulation and Computation*, 23:157–164, 1994.

A Mixture Simulation Algorithm

Table 9 gives the algorithm that we used to simulate a single vMF distribution. Table 8 gives the algorithm used to simulate a mixture of vMF distributions with given parameters. The algorithm in Table 8 makes use of the algorithm in Table 9, which has been adapted from [Woo94].

```
function mixsamp($n$, $d$, $M$)
In: $n$ points to sample; $d$ dimensionality, $M$ mixture data structure
Out: $M$ modified mixture, $L$ label of each sampled point.

1. $L \leftarrow$ zeros(n,1);
2. $P \leftarrow$ rand(1,n);
3. $\mathcal{X} \leftarrow$ zeros(n,d);
4. $cp \leftarrow 0$;          {Cumulative sum of priors}
5. $cs \leftarrow 0$;          {Cumulative sum of number of sampled points}
6. for $j \leftarrow 1$ to $k$
       $ns \leftarrow \text{sum}(P \geq cp$ and $P < cp + M.P(\omega_j))$;
       $\kappa \leftarrow M.\kappa(j)$;
       $\mathcal{X}(ns+1 : cs+ns, :) \leftarrow \text{vsamp}(M.\boldsymbol{\mu}_j, \kappa, ns)$;
       $L(cs+1 : cs+ns) \leftarrow j$;
       $cp \leftarrow cp + M.P(\omega_j)$;
       $cs \leftarrow cs + ns$;
7. end
8. $M.\mathcal{X} \leftarrow \mathcal{X}$
```

Table 8: Simulating a mixture of vMFs

B Mathematical Details

For large values of κ the following approximation is well known [AS74]

$$I_r(\kappa) \approx \frac{1}{\sqrt{2\pi\kappa}} e^{\kappa} \left(1 - \frac{4r^2 - 1}{8\kappa}\right). \tag{B.1}$$

```
**function** vsamp($\boldsymbol{\mu}, \kappa, n$)
{Adapted from [Woo94]}
In: $\boldsymbol{\mu}$ mean vector for vMF, $\kappa$ parameter for vMF
In: $n$, number of points to generate
Out: $S$ the set of $n$ vMF($\boldsymbol{\mu}, \kappa$) samples

1. $d \leftarrow \dim(\boldsymbol{\mu})$
2. $t_1 \leftarrow \sqrt{4\kappa^2 + (d-1)^2}$
3. $b \leftarrow (-2\kappa + t_1)/(d-1)$
4. $x_0 \leftarrow (1-b)/(1+b)$
5. $S \leftarrow \text{zeros}(n, d)$

6. $m \leftarrow (d-1)/2$
7. $c \leftarrow \kappa x_0 + (d-1)\log(1-x_0^2)$
8. **for** $i \leftarrow 1$ **to** $n$
       $t \leftarrow -1000$
       $u \leftarrow 1$
       **while** $(t < \log(u))$
           $z \leftarrow \beta(m, m)$      {$\beta(x, y)$ gives a beta random variable}
           $u \leftarrow$ rand          {rand gives a uniformly distributed random number.}
           $w \leftarrow \frac{(1-(1+b)z)}{(1-(1-b)z)}$
           $t \leftarrow \kappa w + (d-1)\log(1-x_0 w)$
       **end**
       $\mathbf{v} \leftarrow \text{urand}(d-1)$       {urand($p$) gives a $p$-dim vector from unif. distr on sphere.}
       $\mathbf{v} \leftarrow \mathbf{v}/\|\mathbf{v}\|$
       $S(i, 1:d-1) \leftarrow \sqrt{1-w^2}\mathbf{v}^T$
       $S(i, d) = w$
9. **end**

{ We now have $n$ samples from $M_d([0\ 0\ \dots\ 1]^T, \kappa)$ }
10. Perform an orthogonal transformation on each sample in $S$.
    The transformation has to satisfy $Q\boldsymbol{\mu} = [0\ 0\ \dots\ 1]^T$
11. **return** $S$.
```

Table 9: Algorithm to simulate a vMF

Using (B.1) we obtain

$$A_d(\kappa) \approx \left(1 - \frac{d^2-1}{8\kappa}\right)\left(1 - \frac{(d-2)^2-1}{8\kappa}\right)^{-1}. \tag{B.2}$$

Now using the fact that κ is large, expanding the second term using its Taylor series and ignoring terms with κ^2 or more in the denominator we are left with:

$$A_d(\kappa) \approx \left(1 - \frac{d^2-1}{8\kappa}\right)\left(1 + \frac{(d-2)^2-1}{8\kappa}\right). \tag{B.3}$$

On again ignoring terms containing κ^2 in the denominator we finally have

$$A_d(\kappa) \approx 1 - \frac{d-1}{2\kappa}\cdot \tag{B.4}$$

Hence for large κ we can solve $A_d(\kappa) = \bar{R}$ to obtain:

$$\kappa \approx \frac{\frac{1}{2}(d-1)}{1-\bar{R}}\cdot \tag{B.5}$$

We can write $I_r(\kappa)$ as [AS74],

$$I_r(\kappa) = \sum_{k\geq 0} \frac{1}{\Gamma(k+r+1)k!}\left(\frac{\kappa}{2}\right)^{2k+r}, \tag{B.6}$$

where $\Gamma(x)$ is the Gamma function from calculus. So for small κ we use only the first two terms of this series and ignore terms with higher powers of κ to get

$$I_r(\kappa) \approx \frac{\kappa^r}{2^r\, r!} + \frac{\kappa^{2+r}}{2^{r+2}\,(1+r)!}\cdot \tag{B.7}$$

Hence on simplifying $A_d(\kappa)$ we obtain

$$A_d(\kappa) \approx \frac{\kappa}{d}, \tag{B.8}$$

so that

$$\kappa \approx d\bar{R}. \tag{B.9}$$

These estimates for κ do not really take into account the dimensionality of the data and thus for high dimensions (when κ is big by itself but κ/d is not very small or very big) these estimates fail. Note that $A_d(\kappa)$ is a ratio of Bessel functions that differ in their order by just one, so we can use a well known continued fraction expansion for representing $A_d(\kappa)$. For notational simplicity let us write the continued fraction expansion as:

$$A_{2s+2}(\kappa) = \frac{I_{s+1}}{I_s} = \frac{1}{\frac{2(s+1)}{\kappa}+}\;\frac{1}{\frac{2(s+2)}{\kappa}+}\cdots\;. \tag{B.10}$$

The continued fraction on the right is well known [Wat96]. Equation (B.10) and $A_d(\kappa) = \bar{R}$, allow us to write:

$$\frac{1}{\bar{R}} \approx \frac{2(s+1)}{\kappa} + \bar{R}.$$

Thus we can solve for κ to obtain the approximation,

$$\kappa \approx \frac{(2s+2)\bar{R}}{\bar{R}-\bar{R}^2}. \tag{B.11}$$

Since we made an approximation above, we incur some error, so we add a correction term (determined empirically) to the approximation of κ and obtain Equation (B.12).

$$\hat{\kappa} = \frac{\bar{R}d - \bar{R}^3}{1 - \bar{R}^2} \tag{B.12}$$

The above approximation can be generalized to include higher order terms in $\bar{R}$ to yield more accurate answers.[5] For $d = 2, 3$ highly accurate approximations can be found in [Hil81]. For more details and derivations related to the calculation of κ, please refer to [DS03].

C Normalized Mutual Information plots

In this section we have included all the plots given in the main text, but this time the mutual information values have been normalized using a Max Entropy normalization [SGM00] that is defined as

$$\text{NMI}(X, Y) = \frac{2I(X, Y)}{\ln k + \ln c}, \qquad |X| = k, |Y| = c.$$

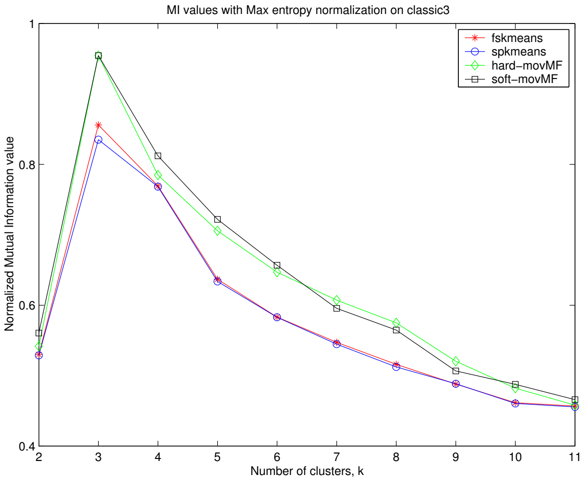

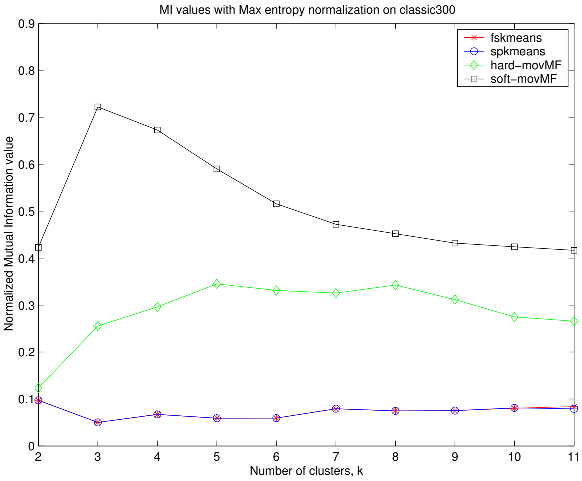

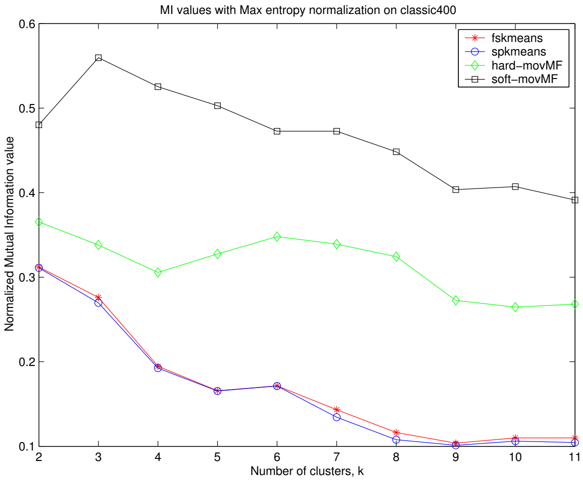

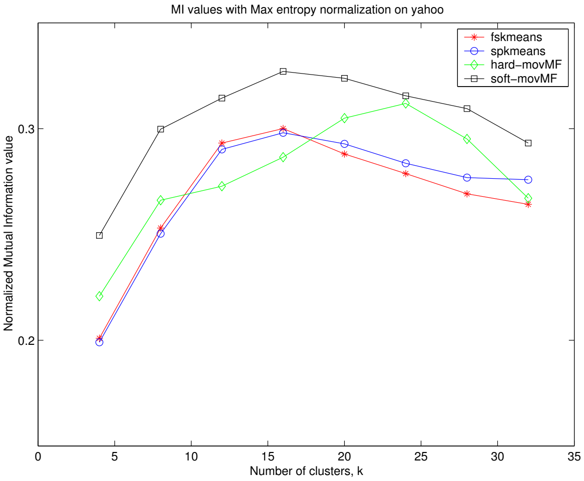

[5] Note that if one really wants more accurate approximations, it is better to use (B.12) as a starting point and then perform a couple of Newton-Raphson iterations, because it is easy to evaluate $A_d'(\kappa) = 1 - A_d(\kappa)^2 - \frac{d-1}{\kappa} A_d(\kappa)$.

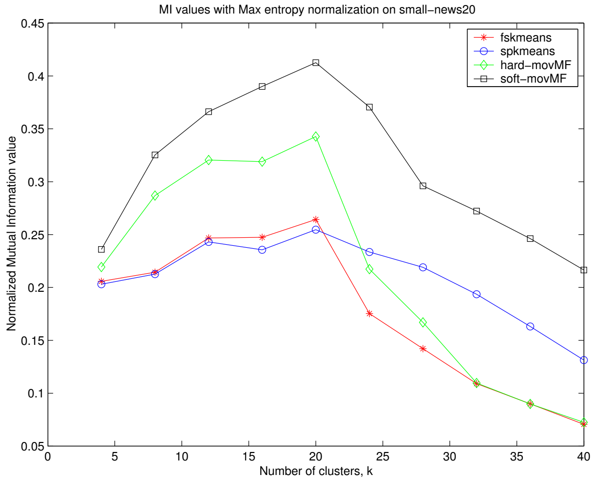

MI values with Max entropy normalization on small−news20

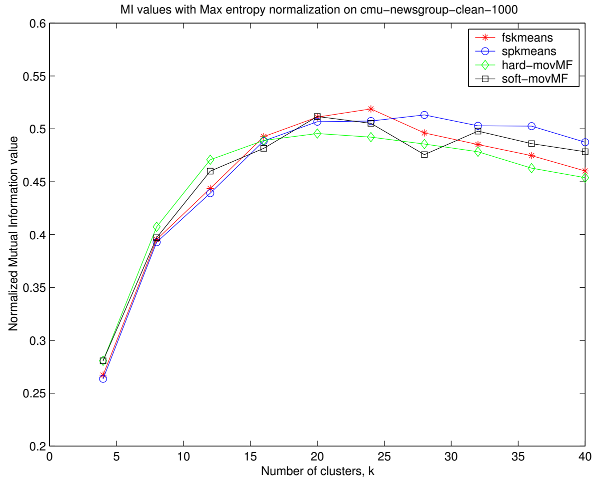

MI values with Max entropy normalization on cmu−newsgroup−clean−1000

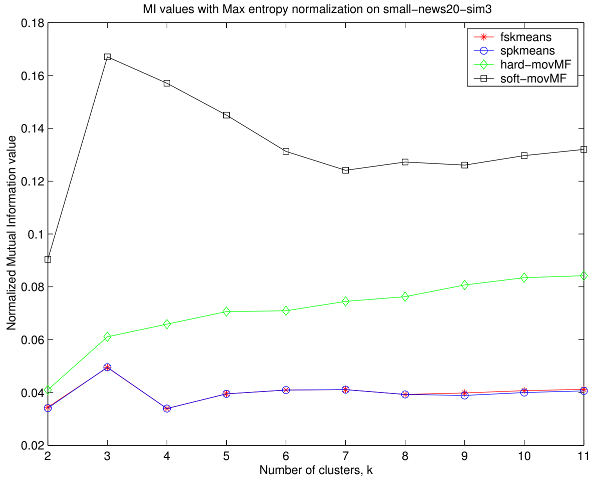

MI values with Max entropy normalization on small−news20−sim3

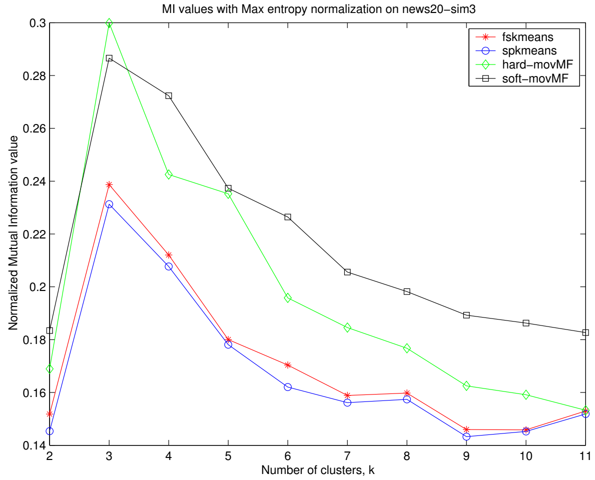

MI values with Max entropy normalization on news20−sim3

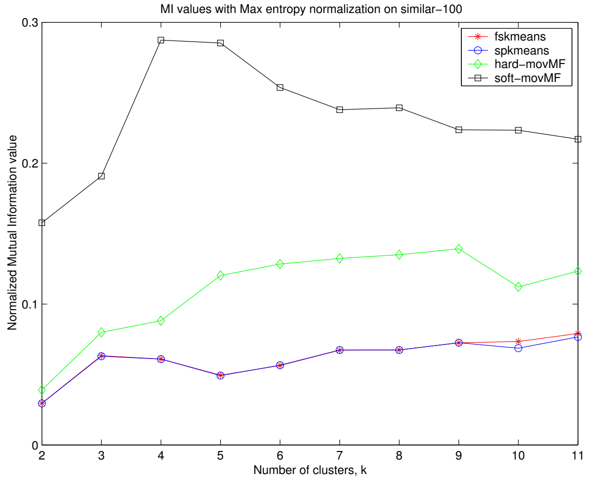

MI values with Max entropy normalization on similar−100

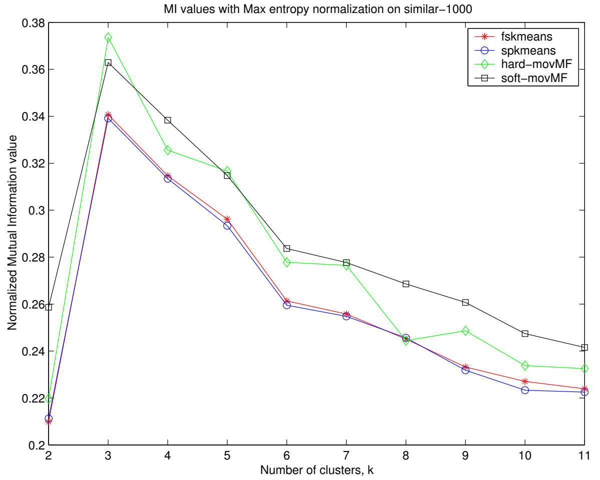

MI values with Max entropy normalization on similar−1000

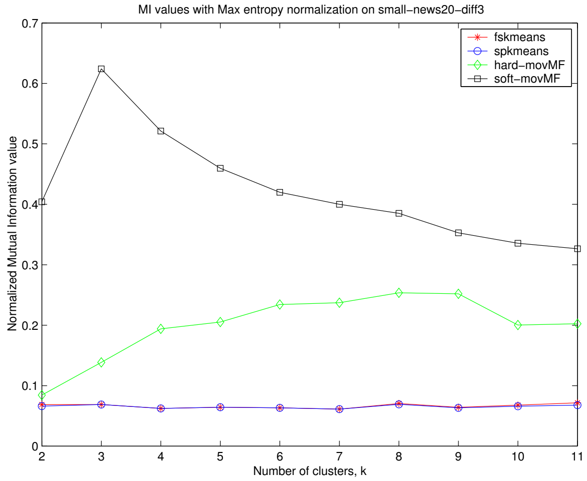

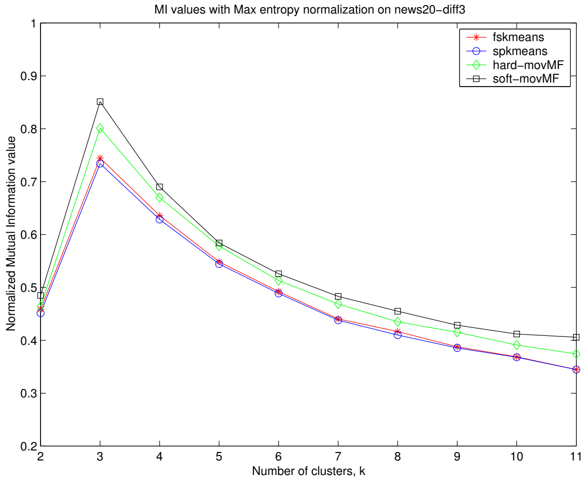

A notable thing about the normalized mutual information plots is that most of the values peak at the true number of clusters for almost all datasets and algorithms. This is a desirable feature and this particular normalization brings it to the fore.